Adsorption 10: 159–185, 2004

Incremental Gravimetry: A Method for Two-Parameter Model Building of Binary Gas Co-Adsorption Equilibria

D. TONDEUR*, K. BONNOT AND L. LUO
Laboratoire des Sciences du Génie Chimique—CNRS ENSIC-INPL Nancy, France
tondeur@ensic.inpl-nancy.fr

Received May 2, 2003; Revised February 10, 2004; Accepted March 29, 2004

Abstract. This paper presents and develops a novel methodology to determine thermodynamic parameters of binary gas co-adsorption equilibria at given total pressure, based *exclusively* on binary gravimetric measurements at this same total pressure, together with single component isotherms. By "Incremental Gravimetry", we designate a procedure in which the adsorbent sample is submitted to increments of composition of a flowing binary gas, and the corresponding increments of weight of the sample at equilibrium are measured. The experimental example is the co-adsorption of methane and carbon dioxide on Norit activated carbon near ambient temperature and pressure.

The approach relies on the thermodynamics of non-ideal adsorbed solutions. The experimental methodology is described, the underlying theory is then presented. Compact analytical expressions are established that relate the measured limiting slopes of the incremental gravimetric curves (at infinite dilution of one component in the other) to quantities that derive only from the pure component isotherms, and to the infinite dilution activity coefficients. The latter are then uniquely determined. Classical two-parameter models for the composition dependence of activity coefficients are then implemented to reconstruct the complete binary isotherms and the incremental gravimetric curves. The comparison of the latter with the measured curves permits to test the different models.

Keywords: co-adsorption, gravimetry, IAS, non-ideal solution, activity coefficients

Introduction

The present work was motivated by the need for a predictive approach to multi-component adsorptive equilibria (multi-meaning more than two) in the simulation of gas purification processes. The most classical approaches, for vapour-liquid equilibrium for example, rely on the multi-component extension of binary properties. In such a framework, it is in principle sufficient to measure single component properties and some characteristic binary quantities, and then to incorporate these data into a coherent and possibly general thermodynamic model suitable for multi-component extension. The present work was therefore oriented toward the building of the theoretical model directly and simultaneously with an experimentally simple measurement, and the use of a theoretical framework that allows extension to multicomponent systems from binaries.

Microbalance weight measurement is a classical technique for the determination of *single component* gas phase adsorption isotherms. The weight change of the adsorbent sample gives directly the increment in adsorbed quantity corresponding to an applied change in partial pressure of the adsorbed species. The convenience and precision of the weight measurements motivate the extension of their principle to mixture adsorption. However, when more than one component is adsorbed, the weight variation alone does not *a priori* furnish enough information to discriminate between the different components. The most direct approach is then to desorb the adsorbed components into an evacuated container and to analyse the content, thus obtaining

*To whom correspondence should be addressed.

direct information on the adsorbed phase composition. This procedure is burdensome and not necessarily accurate. A classical alternative (Do, 1998) is to simultaneously measure the composition variation of the gas phase in a batch equilibration process, and to retrieve the adsorbed quantities of each component from a material balance over the equilibration process. However simple this procedure appears, it introduces imprecision due to the sampling and analysis of the gas phase and of course, it requires time and investment for the analytical device. Powerful alternatives have been developed by Keller and co-workers, based on measuring *simultaneously* the mass adsorbed and the density of the gas phase, or on simultaneous gravimetric and volumetric measurements (Keller et al., 1999; Dreisbach et al., 2001). In these procedures, the chemical analysis of the gas phase is replaced by an additional physical measurement, which may be automated.

All the preceding methods are direct measurements independent of any model, and even of any thermodynamic assumption. If modelling for simulation is the goal, some postulated models have to be fitted to the results thus obtained, and the choice of models and of fitting method is left open. A different philosophy of approach arises when one assumes that the adsorbed phase actually behaves like a macroscopic phase, and thus satisfies thermodynamic constraints, such as the Gibbs adsorption isotherm and the Gibbs-Duhem constraint. These constraints are *in principle* sufficient to render the measurement of the adsorbed phase composition unnecessary.

Such an approach was proposed by Van Ness (1969) to obtain the adsorbed phase composition, together with the spreading pressure, from information on the *total adsorbed amount at different total pressures*, using an iterative numerical calculation. Although this method is consistent and saves a considerable amount of time and equipment, it has been little used so far, may be because it is considered as a model dependent fitting method, that may lead to equivocal results. Actually, the only model assumptions involved in this approach are those of the Gibbs isotherm, applying classical thermodynamics to the gas/adsorbed phase equilibrium. While this approach may be inappropriate when the adsorbate does not really form a "phase," or when steric effects arise, as in the cages of zeolites, it can be reasonably and widely used and is the background of all approaches based on the Adsorbed Solution Theory (Myers and Prausnitz, 1965). Using the Van Ness method, Van der Vaart (Van der Vaart et al., 2000) determined binary co-adsorption isotherms of methane and carbon dioxide on activated carbon Norit RB1, and we shall use an almost identical system here (with Norit RB2 instead). The same gas mixture was investigated using the same approach by Buss (1995) with another carbon. A few other references are to be found (Friederich and Mullins, 1972; Myers et al., 1982) with different systems.

A similar approach, also based on gravimetric measurements at different pressures but with a different numerical solution, was proposed by Myers (1989). He mentions that about 100 experimental points are required for a good precision, and subsequently proposes a method that requires less data, but involves an explicit model for the excess Gibbs energy as a function of composition and spreading pressure. The three parameters of this model are found by minimization of the deviation of the experimental and calculated total adsorbed mass. This method furnishes the parameters of a model together with the composition of the adsorbed phase, it is therefore not a direct measurement, but rather what we call a model-building approach. It showed excellent results for systems involving CO_2, C_3H_8 and H_2S on H-mordenite.

The present paper proposes an alternative approach, based on the same experimental instrument (weight measurements), and the same thermodynamic premises (the Adsorbed Solution Theory) but with a different methodology. The difference with the above approaches is that it seeks to avoid parameter fitting and optimization, and to have instead univocal algebraic determinations of the thermodynamic parameters which are the infinite dilution activity coefficients. In addition, measurements at different pressures are not needed for a given isotherm. As in Myers' approach, the adsorbed phase composition is obtained indirectly. The method partly relies on a detailed thermodynamic analysis developed for chromatographic experiments and presented in a previous publication related to chromatography (Kabir et al., 1998). In contrast to the Van Ness approach, the thermodynamic equations are treated analytically, and no iterative numerical resolution is needed.

Let us first briefly summarize Van Ness' method as presented by Van der Vaart (2000). It starts from a particular form of the Gibbs adsorption isotherm which is written at constant T:

$$-\frac{1}{q_t}d\psi + d\ln P + \sum x_i d\ln y_i = 0 \qquad (1)$$

where x_i and y_i are respectively the adsorbed phase and the gas phase mole fractions, q_t is the total adsorbed concentration (moles adsorbed $\cdot$ kg^{-1} of adsorbent), P is total pressure, and ψ is a quantity called "loading" by Myers, because it has dimensions of (moles$\cdot$kg^{-1}), and called "compressibility factor" by Van Ness, because it is related to the spreading pressure Π by a relation analogous to a state equation for gases:

$$\psi = \frac{\Pi A}{RT} \tag{2}$$

where A is the specific surface of the adsorbent (m^{2}kg^{-1}). At constant composition and T, Eq. (1) yields a relation between loading and pressure:

$$\left(\frac{\partial \psi}{\partial P}\right)_{T,y} = \frac{q_t}{P} \tag{3}$$

which is integrated into:

$$\psi = \int_0^P \frac{q_t}{P} dP \tag{4}$$

We relate q_t to the total adsorbed mass m_t, equal to the mass w given experimentally by the balance minus the mass m_a of the clean adsorbent sample. Using the average molar mass of the mixture M:

$$M = \sum x_i M_i \tag{5}$$

the following relation holds between these quantities:

$$q_t = \frac{m_t}{M \cdot m_a} \tag{6}$$

At constant P and T, Eq. (1) yields a relation between loading and composition:

$$-\frac{1}{q_t} d\psi + \sum \frac{x_i}{y_i} dy_i = 0 \tag{7}$$

or for a binary case:

$$x = y + \frac{My(1-y)}{m_t}\left(\frac{\partial \psi}{\partial y}\right)_{P,T} \tag{8}$$

For a given gas phase composition y, Eqs. (4)–(6) and (8) are solved simultaneously by an iterative numerical method for the unknown variables ψ, M and x. Owing to Eq. (4), the experimental adsorbed mass must be determined at different total pressures for given gas compositions, between which interpolation can be performed. The method can therefore be considered as a global and thermodynamically consistent fitting method rather than a direct measurement. Once the compositions of the two phases in equilibrium are determined, they can be used to adjust an explicit model, for example to fit the parameters of an explicit binary isotherm equation, or to calculate activity coefficients in a non-ideal adsorption solution model. Notice also that the input of the single component isotherms is required only when an explicit model is to be designed.

By contrast, the approach proposed here uses the single component isotherms as input data, and requires binary measurements only at the total pressure where the binary equilibrium is established.

The Experimental Operating Mode and Methodology

The experimental set-up, shown schematically on Fig. 1, is basically a micro-thermo-balance (Rubotherm, Bochum, Germany) associated to a system for generating and circulating continuously gas or vapour mixtures. The binary compositions are adjusted using mass-flow-meters. Classically, the adsorbent sample, contained in the measuring cell, is conditioned at high temperature under vacuum, and weighed after return to the working temperature, giving the mass of clean adsorbent m_a. The adsorbent is then submitted to a flow of a single component, labelled 1, until equilibrium is achieved (weight stabilised, temperature returned to the specified value). This will constitute the initial or background equilibrium state of the experiment and it is also a point of the adsorption isotherm of component 1. The mass then measured is the sum of the mass of the adsorbent m_a and of the adsorbed component m_1°. Here, the subscript 1 designates the adsorbed component, and the superscript 0 indicates the initial state.

Next, the composition of the incoming gas flow is slightly changed ("perturbed", or incremented) by adding a small flow-rate of component 2, while keeping constant the total pressure in the measuring cell. This is equivalent to a small change in partial pressure of the components. After returning to equilibrium, the measured mass has undergone a small variation δm. From this unique information, and the knowledge of the single component isotherms, we shall show how to extract a value of the activity coefficient of component

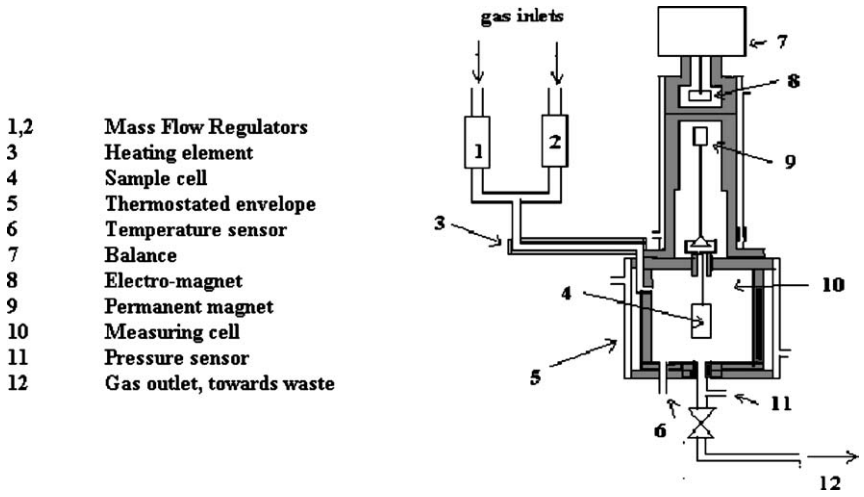

Figure 1. Experimental set-up of microbalance to measure adsorption equilibria.

2 at infinite dilution in component 1 in the adsorbed phase.

This new equilibrium state, now entirely defined, is then the new initial state, and the procedure can be repeated with a new change in composition, that is of partial pressures, until the full range of the binary composition is covered. We thus obtain a curve of the total adsorbed mass m_t versus composition of the gas phase. At the other end of the composition interval, the initial experiment is repeated with components 1 and 2 interchanged, so that the infinite dilution activity coefficient of component 1 in component 2 is obtained. It is recommended to run the whole experiment "backwards", that is with increasing concentration of component 1, as a cross-check.

The experiment may be carried out in a continuous-flow mode, or in a discontinuous mode, in which the flow through the cell is interrupted while the weight measurement is taken. The latter procedure may also generate slight perturbations, and we found the continuous mode finally more reliable, providing it is operated slow enough (to avoid aerodynamic effects) and sufficient time is allowed for relaxation of the signal after each composition change. We considered the best overall test for attainment of equilibrium is the relative coincidence of the forward and backward curves.

We emphasize that only total weight measurements are done, no further information on the gas phase is required, providing its composition defining each equilibrium state is established with good accuracy. As we shall see now, the use of this approach requires the use of a general thermodynamic model of the adsorbed phase.

Theoretical Development

Information from the Weight Measurement

Let us first formalise the information obtained from the single incremental experiment described above, in the general case where the initial equilibrium state involves the two adsorbed components. This initial state is assumed to be known. Let m_t° be the total mass adsorbed measured, in this initial state, with

$$m_t^\circ = m_1^\circ + m_2^\circ \tag{9}$$

Let us introduce the concentrations q in the adsorbed phase, such that

$$q_t = q_1 + q_2 = \frac{m_1}{m_a M_1} + \frac{m_2}{m_a M_2} \tag{10}$$

where M_1 and M_2 are the molar masses of the adsorbed components (kg·mol^{-1}), and the adsorbed concentrations q_i are expressed in (mol · kg^{-1} adsorbent). The mole fractions in the adsorbed phase are such that:

$$x_i = q_i/q_t \tag{11}$$

$$x_1 + x_2 = 1 \tag{12}$$

The composition increment leads to changes in all these variables, and we designate by δz the variation between the new state z and the initial state z° of any variable z. For small changes the measured mass change δm is then:

$$\delta m_t = m - m^\circ = \delta m_1 + \delta m_2 = m_a[M_1\delta q_1 + M_2\delta q_2] \tag{13}$$

together with

$$\delta q_i = \delta(x_i q_t) = x_i^\circ \delta q_t + q_t^\circ \delta x_i \tag{14}$$

and

$$\delta x_1 + \delta x_2 = 0 \tag{15}$$

We shall now refer all the changes δz to one of them, selected as the partial pressure of component 1, that is, to δp_1. Substituting Eq. (14) into Eq. (13) and using Eqs. (5) and (15), we obtain:

$$\frac{1}{m_a}\frac{\delta m_t}{\delta p_1} = M^\circ \frac{\delta q_t}{\delta p_1} + q_t^\circ (M_1 - M_2)\frac{\delta x_1}{\delta p_1} \tag{16}$$

Keeping in mind that δm_t is a measured quantity and that the initial state (superscripts 0) is known, Eq. (16) is a first relation between the two unknowns $\delta q_t/\delta p_1$ and $\delta x_1/\delta p_1$. We now need to establish a second relation between these two unknowns, independent of Eq. (16). For this purpose, thermodynamic modelling of the adsorbed phase is necessary.

Existence of a Thermodynamic Relation Between $\delta q_t/\delta p_1$ and $\delta x_1/\delta p_1$

A common binary adsorption equilibrium (without hysteresis) can be represented, at constant temperature and total pressure, as shown on the experimental examples of Figs. 5 and 8 which will be presented later.

The adsorbed concentrations q_1 and q_2 and thus the total concentration q_t, depend only on the partial pressures p_1 and p_2 of the two components, and at constant P, one only of these partial pressures is independent. One can therefore define ordinary derivatives of these variables with respect to p_1. Considering that the change in partial pressure of component 1 is small, the variations can be assimilated to the first derivatives with respect to this partial pressure:

$$\frac{\delta m}{\delta p_1} \to \frac{dm}{dp_1}; \quad \frac{\delta q_t}{\delta p_1} \to \frac{dq_t}{dp_1}; \quad \frac{\delta x_1}{\delta p_1} \to \frac{dx_1}{dp_1} \tag{17}$$

For given adsorbent, P, T and species 1 and 2, there is a unique plot such as Fig. 5, where the independent variable has been taken as p_1. Thus to any value of p_1 corresponds a unique set of values of p_2, x_1, x_2, q_1, q_2, q_t, as well as their derivatives with respect to p_1. Thus dq_t/dp_1 and dx_1/dp_1 are not independent, and there must exist a relation between these quantities which is determined only by equilibrium, and therefore independent of Eq. (16). We now proceed to establish algebraically this relation, starting from rather general thermodynamic properties of the adsorbed phase.

Thermodynamics of the Non-Ideal Adsorbed Phase

We start with the now classical Adsorbed Solution Theory, introduced initially by Myers and Prausnitz (1965). This approach parallels liquid-vapour equilibrium, with the difference that the surface tension, or spreading pressure Π, of the adsorbed phase has to be introduced as state variable. The activity coefficients in the adsorbed phase then become a function of the spreading pressure. The constitutive equations of the equilibrium are then (Myers and Prausnitz, 1965; Kabir et al., 1998; Do, 1998), the gas phase being assumed perfect:

$$p_i = P_i^* x_i \gamma_i \tag{18}$$

$$\frac{1}{q_t} = \frac{a_t}{A} = \frac{\sum \bar{a}_i x_i}{A} = \sum \frac{a_i^* x_i}{A} + \frac{1}{A}\left(\frac{\partial g^{\text{ex}}}{\partial \Pi}\right)_{T,x_i}$$

$$= \sum \frac{x_i}{q_i^*} + \sum x_i \left(\frac{\partial \ln \gamma_i}{\partial \psi}\right)_{T,x_i} \tag{19}$$

In Eq. (18), P_i^* is a fictitious pressure, analogous to the vapour pressure of the pure component in vapour-liquid equilibrium: it is the pressure that species i adsorbed alone would exert, at the same P, T and the same spreading pressure Π as the mixture. P_i^* is determined from the single component isotherm of i, as a function of Π. Equation (19) results from the definition of the excess surface $a^{\text{ex}} = \Sigma \bar{a}_i x_i - \Sigma a_i^* x_i$ of the adsorbed phase (two-dimensional analogue of the

excess volume) as the derivative of the excess molar Gibbs energy g^{ex} with respect to spreading pressure Π, and ψ is loading as defined in Eq. (2). $\bar{a}_i$ is the partial molar surface area of species i, a mixture property. The superscript $*$ refers to single component isotherms and will be explained in more detail below (see for example Kabir et al. (1998), or the original paper of Myers and Prausnitz (1965)). q_i^* is the adsorbed concentration of pure i corresponding to the partial pressure $p_i = P_i^*$, also obtained from the pure i isotherm.

In the binary case, the required relation between the derivatives of q_t and of x_1 will be obtained by implicit differentiation of Eqs. (18) and (19), accounting for Eqs. (10)–(12). An essential special case of the present treatment is that of infinite dilution, for which compact, relatively simple, and rather general solutions are found. In the general case, this calculation requires one to define a model of the excess Gibbs energy, or of the activity coefficients, not only as a function of the composition of the adsorbed phase (x_1, x_2), but also as a function of spreading pressure, or of loading ψ. Before doing this in a general fashion, we shall consider some limiting cases, for which the calculations will serve as illustrations, and the result of which will also prove useful in the general cases.

Calculation of dq_t/dp_1 in the ideal case (IAS Framework)

When the adsorbed phase is considered ideal, the excess Gibbs energy is zero, and the second term in Eq. (19) disappears. The calculation of the derivative of q_t then proceeds as follows:

$$\begin{aligned}\frac{dq_t}{dp_1} &= -q_t^2 \frac{d}{dp_1}\left(\frac{1}{q_t}\right) = -q_t^2 \frac{d}{dp_1}\left[\frac{x_1}{q_1^*} + \frac{1-x_1}{q_2^*}\right] \\ &= -q_t^2\left[\frac{1}{(q_1^*)^2}\left(q_1^* \frac{dx_1}{dp_1} - x_1 \frac{dq_1^*}{dp_1}\right)\right. \\ &\quad \left. + \frac{1}{(q_2^*)^2}\left(-q_2^* \frac{dx_1}{dp_1} - x_2 \frac{dq_2^*}{dp_1}\right)\right] \end{aligned} \tag{20}$$

The derivatives of q_i^* appearing in Eq. (20) are obtained from the single component isotherms, and can be considered as depending on P_i^* alone. Thus one may write

$$\frac{dq_i^*}{dp_1} = \frac{dq_i^*}{dP_i^*}\frac{dP_i^*}{dp_1} \tag{21}$$

$$\frac{dP_i^*}{dp_1} = \frac{d}{dp_1}\left(\frac{p_i}{x_i}\right) = \frac{1}{x_i}\frac{dp_i}{dp_1} - \frac{P_i^*}{x_i}\frac{dx_i}{dp_1} \tag{22}$$

The derivatives of P_i^* are obtained from Eq. (18) with $\gamma_i = 1$. Substituting Eqs. (21) and (22) into Eq. (20), and after some rearrangements, one obtains:

$$\begin{aligned}-\frac{1}{q_t^2}\frac{dq_t}{dp_1} &= \frac{dx_1}{dp_1}\left[\frac{1+\xi_1^*}{q_1^*} + \frac{1+\xi_2^*}{q_2^*}\right] \\ &\quad - \frac{\xi_1^*}{q_1^* P_1^*} - \frac{\xi_2^*}{q_2^* P_2^*}\end{aligned} \tag{23}$$

where

$$\xi_i^* = \frac{P_i^*}{q_i^*}\frac{dq_i^*}{dP_i^*} \tag{24}$$

ξ_i^* is a parameter depending only on the single component isotherm of which it measures the concavity (the isotherm is concave toward the p axis for $\xi_i . < 1$). Equation (23) is the sought relation between the derivatives of q_t and of x_1.

The Infinite Dilution Limiting Case ($x_1^\circ \to 0$)

This limiting case corresponds to the initial starting point of the experimental procedure. The limit values of the different variables are, when $x_1 \to 0$:

$$\begin{aligned} &x_2^\circ \to 1; \quad p_2 \to P; \quad P_2^* \to P; \\ &q_t \to q_{2\,\mathrm{lim}} = q_2^*(P); \quad M \to M_2 \end{aligned}$$

The fictitious pressure P_1^* tends toward a non-zero limit value, which we designate by $P_{1,\mathrm{lim}}^*$. The corresponding value of q_1^* is $q_{1,\mathrm{lim}}^* = q_1\,(P_{1,\mathrm{lim}}^*)$. The concavity parameters ξ_i^* then also tend toward some finite limit value; for example:

$$\xi_{1\,\mathrm{lim}}^*(x_1 \to 0) = \frac{P_{1\,\mathrm{lim}}^*}{q_1^*(P_{1\,\mathrm{lim}}^*)}\left(\frac{dq_1}{dp_1}\right)_{x_1=0} \tag{25}$$

Equation (23) thus remains valid, with all quantities taking up their limit value. Equation (16) may be rewritten in terms of derivatives with respect to p_1 instead of variations:

$$\begin{aligned}\frac{1}{m_a}\left(\frac{dm}{dp_1}\right)_{x_1=0} &= M_2\left(\frac{dq_t}{dp_1}\right)_{x_1=0} \\ &\quad + q_2^*(P)[M_1 - M_2]\left(\frac{dx_1}{dp_1}\right)_{x_1=0}\end{aligned} \tag{26}$$

When Eqs. (23) and (26) are combined to eliminate dq_t/dp_1 for example, a relation is obtained between

the measured quantity dm_t/dp_1 and the composition change dx_1/dp_1 of the adsorbed phase. On the other hand, since we are in the framework of the Ideal Adsorbed Solution Theory, dx_1/dp_1 can be calculated analytically (Kabir et al., 1998, Appendix) as:

$$\left(\frac{dx_1}{dp_1}\right)^{\text{IAS}}_{x_1=0} = \frac{1}{P^*_{1\,\text{lim}}} \tag{27}$$

Finally, the complete explicit expression for dm_t/dp_1, in the IAS framework, is:

$$\frac{1}{m_a}\left(\frac{dm_t}{dp_1}\right)^{\text{IAS}}_{x_1=0} = \frac{q^*_2(P)}{P^*_{1\,\text{lim}}}\left[M_1 - M_2{}^{\text{IAS}}\right] \tag{28}$$

where:

$$M'^{\text{IAS}}_2 = M_2\left[\frac{q^*_2(P)}{q^*_{1\,\text{lim}}} - \xi^*_{2\,\text{lim}}\left(1 - \frac{P^*_{1\,\text{lim}}}{P}\right)\right] \tag{29}$$

Practical Use and Validation

We are now in possession of two values of (dm_t/dp_1) at $x_1 = 0$: a measured value on one hand, and on the other hand a theoretical value calculated using Eq. (28) and the single component isotherms, in the IAS framework. A similar procedure may then be followed to obtain such values at the other end of the composition interval, that is, for $x_2 \to 0$. One question is how small the increment of composition should be to allow assimilation with the derivative. A way to circumvent this question is to extrapolate the curve obtained with successive increments.

The coincidence of measured and IAS values at each end of the composition interval furnishes a good test of validity of the IAS model. Of course, this validity may be tested more fully by using measurements all along the composition interval. We shall see later on an example how this is handled. But the interest of the IAS approach is not uniquely as a test. When deviations occur between calculated and measured values, they are a measure of non-ideality, and it is of interest to determine whether some "non-ideality" coefficients, such as activity coefficients, may be retrieved from these deviations.

This non-ideal approach can only be developed in a somewhat broader thermodynamic framework. The Regular Solution Theory is such a framework. We illustrate this first with the so-called Real Adsorbed Solution (RAS) model.

The Regular-Adsorbed-Solution Model

The Regular Solution Theory relies on two basic assumptions, namely that the excess entropy of mixing S^{ex} is zero, and that the volume of mixing V^{ex} is zero. But the excess Gibbs energy G^{ex} is non-zero, implying that the activity coefficients differ from 1:

$$S^{\text{ex}} = -(\partial G^{\text{ex}}/\partial T)_{P,x} = 0 \tag{30}$$

$$V^{\text{ex}} = V^{\text{mix}} = 0 \tag{31}$$

$$G^{\text{ex}} = nRT\Sigma x_i \ln \gamma_i \neq 0 \tag{32}$$

The condition on entropy Eq. (30), implies that the model used for the excess Gibbs energy is temperature independent, and we shall be referring to this situation in some models used below. Note also that the transposition from solution theory to adsorbed solution theory implies that the derivative in the first equation above be taken at constant spreading pressure Π instead of constant pressure P.

In the so-called Real Adsorbed Solution (RAS) model (Costa et al., 1981) the adsorbed phase is non-ideal, in the sense that it obeys Eq. (18) with $\gamma_i \neq 1$. However, the activity coefficients are considered independent of the spreading pressure, and dependent only on composition (x_1, x_2). This is equivalent to saying that the excess surface is zero, i.e. that the surface area of the adsorbed phase is the sum of the surface areas of the separate components at the same temperature and spreading pressure. The second term in Eq. (19) therefore cancels. This assumption is analogous to assuming a zero excess mixing volume V^{ex} in a three-dimensional phase, i.e. one of the assumption underlying the Regular Solution Theory, Eq. (31). The other assumption ($S^{\text{ex}} = 0$) will not be used here, and is therefore not necessary. From now on, we shall refer to the RAS model, designating both the Real Adsorbed Solution model and the Regular Adsorbed Solution model.

The implicit differentiation of Eqs. (18) and (19) follows the same lines as in the ideal case, and has been developed in Kabir et al. (1998). Thus only the end result is given here:

$$\frac{dx_1}{dp_1} = \frac{1}{1+\Delta}\left[\frac{q_1}{\gamma_2 P^*_2 q^*_1} + \frac{q_2}{\gamma_1 P^*_1 q^*_2}\right] \tag{33}$$

$$-\frac{1}{q_t^2}\frac{dq_t}{dp_1} = \frac{dx_1}{dp_1}\left[\frac{1+\xi_1^*(1+\Delta)}{q_1^*} - \frac{1+\xi_2^*(1+\Delta)}{q_2^*}\right] - \frac{\xi_1^*}{\gamma_1 P_1^* q_1^*} - \frac{\xi_2^*}{\gamma_2 P_2^* q_2^*} \tag{34}$$

with

$$\Delta = x_1\left(\frac{\partial \ln\gamma_1}{\partial x_1}\right)_T = x_2\left(\frac{\partial \ln\gamma_2}{\partial x_2}\right)_T \tag{35}$$

The equality of the two terms in Eq. (35) results from the Gibbs-Duhem constraint.

These equations involve quantities calculable from the single component isotherms (bearing the superscript *), but also involve the activity coefficients and their dependence on composition. Before introducing the appropriate models for this, let us again consider the starting point of the procedure, the limiting case of infinite dilution.

Limiting Case of Infinite Dilution ($x_i^\circ \to 0$)

When $x_1 \to 0$, the quantities involved tend toward the following limits, some of which have already been mentioned in the IAS case:

$$x_1 \to 0; \quad p_1 \to 0; \quad q_1 \to 0; \quad x_2 \to 1; \quad p_2 \to P;$$
$$P_2^* \to P; \quad q_2 \to q_2^* = q_2^*(P); \quad P_1 \to P_{1\,\mathrm{lim}}^*;$$
$$q_1^* \to q_1^*(P_{1\,\mathrm{lim}}^*); \quad \gamma_1 \to \gamma_1^\infty; \quad \gamma_2 \to 1;$$

γ_1^∞ is the so-called infinite dilution activity coefficient. In addition, because $\partial \ln \gamma_1/\partial x_1$ in principle does not become infinite when $x_1 \to 0$, we have

$$\mathrm{Lim}\Delta(x_1 \to 0) = 0 \tag{36}$$

Because of the equality in Eq. (35), this relation implies that:

$$\frac{\partial \ln \gamma_2}{\partial x_2} \to 0 \quad \text{when } x_1 \to 0.$$

In other words, the Gibbs–Duhem constraint imposes that the pure component activity coefficient approaches the value 1 with zero slope, as the trace component vanishes. With these values, Eq. (33) becomes:

$$\left(\frac{dx_1}{dp_1}\right)_{x_1=0}^{\mathrm{RAS}} = \frac{1}{\gamma_1^\infty P_{1\,\mathrm{lim}}^*} \tag{37}$$

which is to be compared to Eq. (27). The expression for dq_t/dp_1 is Eq. (34) where Δ is made equal to zero, and the variables take the limiting values indicated above. It is interesting to write the expression for dm/dp_1 in a form similar to Eq. (28):

$$\frac{1}{m_a}\left(\frac{dm_t}{dp_1}\right)_{x_1=0}^{\mathrm{RAS}} = \frac{q_2^*(P)}{\gamma_1^\infty P_{1\,\mathrm{lim}}^*}\left[M_1 - M_2'^{\mathrm{RAS}}\right] \tag{38}$$

with

$$M_2'^{\mathrm{RAS}} = M_2\left[\frac{q_2^*(P)}{q_{1\,\mathrm{lim}}^*} - \xi_{2\,\mathrm{lim}}^*\left(1 - \frac{\gamma_1^\infty P_{1\,\mathrm{lim}}^*}{P}\right)\right] \tag{39}$$

One may observe that the relations for the Real Adsorbed Solution can be derived from the ideal case by simply multiplying $P_{1\,\mathrm{lim}}^*$ by γ_1^∞ wherever it occurs.

Practical Use and Validation

The practical use of these equations aims at determining the infinite dilution coefficients from the experiments at $x_1 \to 0$ and $x_2 \to 0$. This is done simply by rearranging Eq. (38) which is a linear form in γ_i^∞

$$\gamma_i^\infty = \frac{R}{Q + \left(\frac{dm_t}{dp_1}\right)_{x_1=0}^{\mathrm{measured}}} \tag{40}$$

with:

$$Q = \frac{m_a}{P} q_2^*(P)\xi_{2\,\mathrm{lim}}^* M_2$$
$$R = \frac{m_a}{P_{1\,\mathrm{lim}}^*} q_2^*(P)\left[M_1 + M_2\left(\xi_{2\,\mathrm{lim}}^* - \frac{q_2^*(P)}{q_{1\,\mathrm{lim}}^*}\right)\right] \tag{41}$$

Q and R include only information on the pure component isotherms.

There is one special case when γ_i^∞ may be calculated more simply: this is when q_t is constant, implying in particular that the adsorbed quantity of the single components at the total pressure P is the same. Then dm/dp_1 is simply related to dx_1/dp_1. In Eqs. (38) and (39), $\tilde{M}_2^{\mathrm{RAS}}$ reduces to M_2 and we find a relation somewhat similar to Eq. (35) of Kabir et al. (1998):

$$\gamma_i^\infty = \frac{(dm/dp_1)^{\mathrm{IAS}}}{(dm/dp_1)^{\mathrm{measured}}} = \frac{m_a q_2^*(P)[M_1 - M_2]}{P_{1\,\mathrm{lim}}^*(dm/dp_1)^{\mathrm{measured}}} \quad (\text{for } q_t = \text{constant})$$

Once the two infinite dilution coefficients γ_1^∞ and γ_2^∞ have been determined, using an experiment at

each end of the composition interval, the equilibrium may be completely described using Eq. (18), Eq. (19) without the spreading pressure term, and a classical two-parameter model for the dependence of activity coefficients on binary composition, such as Wilson, Margules, Van Laar ... We shall illustrate this later with an experimental example.

The validation of the RAS model could be done by using measurements of dm_t/dp_1 in the full composition range, and comparison with the calculated values, using the full Eqs. (33) and (34). But instead of using the derivatives, thus the slopes of the equilibrium curves, a simpler and possibly more useful validation may be done by comparing directly the value of the total mass w measured by the balance to a value calculated by:

$$w = \text{Mass of sample } = m_a(1 + q_1 M_1 + q_2 M_2) \quad (42)$$

where q_1 and q_2 are values calculated using the full model (Eqs. (18) and (19) without the second term and the model chosen for activity coefficients).

It should be kept in mind that in such a procedure, one tests the model chosen for the activity coefficients as well as the RAS approach itself. The possible deviations are due to the combination of these models, of which the contributions may not be identified separately. Any important deviation between model and measurements may be used to develop a more complete thermodynamic model.

The Spreading-Pressure-Dependent Approach (SPD)

The RAS model used in the previous section may be very practical, but from a fundamental point of view, it has the drawback of neglecting a thermodynamically important feature: the effect of spreading pressure on the non-ideality. A more general model is generated when one considers that the activity coefficients are a function of spreading pressure as well as of composition (Talu and Zwiebel, 1986). Thus Eq. (19) has to be considered in its complete form. This model deviates from the Regular Solution Theory in the sense that the excess mixing area is no longer zero.

The calculation of the derivatives dq_t/dp_1 and dx_1/dp_1 has been presented in Kabir et al. (1998, Appendix) and is not repeated here. The resulting formulae resemble Eqs. (33)–(35) but contain additional factors:

$$\frac{dx_1}{dp_1} = \frac{1}{1+\Delta}\left[\frac{q_1(1+\Delta_1)}{\gamma_2 P_2^* q_1^*} + \frac{q_2(1+\Delta_2)}{\gamma_1 P_1^* q_2^*}\right] \quad (43)$$

$$-\frac{1}{q_t^2}\frac{dq_t}{dp_1} = \frac{dx_1}{dp_1}\left[\frac{1}{q_1^*}\left(1+\xi_1^*\frac{1+\Delta}{1+\Delta_1}\right) - \frac{1}{q_2^*}\left(1+\xi_2^*\frac{1+\Delta}{1+\Delta_2}\right)\right] - \frac{\xi_1^*}{q_1^* P_1^* \gamma_1(1+\Delta_1)} \mp \frac{\xi_2^*}{q_2^* P_2^* \gamma_2(1+\Delta_2)} + \frac{dx_1}{dp_1}\left(\frac{\Delta_1}{q_1^*} - \frac{\Delta_2}{q_2^*}\right) + \frac{d\psi}{dp_1}\left(x_1\frac{\partial\Delta_1}{\partial\psi} + x_2\frac{\partial\Delta 2}{\partial\psi}\right) \quad (44)$$

$$\frac{d\psi}{dp_1} = (-1)^i\left[-\frac{q_i^*}{P_i^* x_i \gamma_i(1+\Delta_i)} + \frac{q_i^*}{x_i}\frac{1+\Delta}{1+\Delta_i}\frac{dx_1}{dp_1}\right] \quad (i = 1 \text{ or } 2) \quad (45)$$

with

$$\Delta_i = q_i^*\left(\frac{\partial \ln\gamma_i}{\partial\psi}\right)_{T,x} \quad (46)$$

$$\Delta = x_i\left(\frac{\partial \ln\gamma_i}{\partial x_i}\right)_{T,\psi} \quad (47)$$

Limiting expressions, corresponding to $x_1 \to 0$, may be obtained using reasonable but general assumptions on the model for activity coefficients. We have noticed already that the Gibbs-Duhem requirement that $\Delta_{\lim} = 0$ implies that γ_2 approaches 1 with zero slope in the (γ, x) plane. It is reasonable to assume that this property also applies in the (γ, ψ) plane, implying that:

$$\lim \Delta_2(x_1 \to 0) = \lim q_2\left(\frac{\partial \ln\gamma_2}{\partial\psi}\right)_{T,x} = 0 \quad (48)$$

This assumption is coherent with a generalised Gibbs-Duhem constraint, and is satisfied by the example model which we present below. With these properties, the limiting expressions of the derivatives are:

$$\left(\frac{dx_1}{dp_1}\right)^{\text{SPD}}_{x_1=0} = \left(\frac{dx_1}{dp_1}\right)^{\text{RAS}}_{x_1=0} \quad \text{(see Eq. (37))} \quad (49)$$

$$\frac{1}{m_a}\left(\frac{dm_t}{dp_1}\right)^{\text{SPD}}_{x_1=0} = \frac{q_2^*}{\gamma_1^\infty P_{1\,\lim}^*}\left[M_1 - M_2^{\prime\text{SPD}}\right] \quad (50)$$

Equation (50) has the same form as Eq. (38), but with:

$$M_2'^{\mathrm{SPD}} = M_2\left[\frac{q_2^*(P)}{q_{1\,\mathrm{lim}}^*}(1+\Delta_{1\,\mathrm{lim}}) - [\xi_{2\,\mathrm{lim}}^* - (q_2^*(P))\Delta_2'\left[1-\gamma_1^\infty\frac{P_{1\,\mathrm{lim}}^*}{P}\right]\right] \tag{51}$$

and

$$\Delta_2' = \left(\frac{\partial^2 \ln\gamma_2}{\partial\psi^2}\right)_{T,x_1=0} = \left(\frac{\partial\Delta_2}{\partial\psi}\right)_{T,x_1=0} \tag{52}$$

Equation (51) is to be compared to Eq. (39). A further simplification, to be found in the example model below, is obtained when $\Delta_2' = 0$. In what follows, we illustrate the calculation with what is probably the simplest such model proposed in the literature.

The Iso-Active Sorbent Model of Kopatsis and Myers (ISAC)

Kopatsis (1988) and Siperstein et al. (1999) in the framework of the so-called Iso-Active-Solvent Theory (ISAC) indicate a method of construction of the excess free energy function by combining a classical, composition dependent model (Margules, Van Laar, Wilson...) with an experimental function of loading ψ. Let us illustrate the calculation for a one-parameter Margules equation. The above authors propose, for the molar excess Gibbs energy:

$$g^{\mathrm{ex}} = Bx_1x_2(1-e^{-C\psi}) \tag{53}$$

from which the activity coefficients are calculated by:

$$RT\,\ln\gamma_i = \left(\frac{\partial g^{\mathrm{ex}}}{\partial n_i}\right)_{T,\psi,n_j} = Bx_j^2(1-e^{-C\psi}) \tag{54}$$

The expressions for Δ and Δ_i, from Eq. (46) and (47) and their derivatives appearing in Eq. (44) are calculated as:

$$\Delta_i = \frac{q_i^*BC}{RT}x_j^2e^{-C\psi} \tag{55}$$

$$\left(\frac{\partial\Delta_i}{\partial\psi}\right)_{T,x} = -\frac{q_i^*BC^2}{RT}x_j^2e^{-C\psi} \tag{56}$$

$$\Delta = -\frac{2Bx_1x_2}{RT}(1-e^{-C\psi}) \tag{57}$$

The limit values at infinite dilution of component 1, say, are readily obtained from these expressions. Notice that the property assumed above in the SPD approach, Eq. (48), is satisfied. In addition $\Delta_2'(x_1 = 0) = 0$, implying that the coefficient of $d\psi/dp_1$ in Eq. (44) vanishes, and that Eq. (51) applies in its simplified form.

With these properties, the expressions for the derivatives dx_1/dp_1 and dm_t/dp_1 are identical to Eqs. (37) and (38), but with Eq. (39) replaced by Eq. (51) with $\Delta_2' = 0$. Notice that the only change is the appearance of the term

$$\Delta_{1\,\mathrm{lim}} = \frac{q_{1\,\mathrm{lim}}^*BC}{RT}e^{-C\psi_{1\,\mathrm{lim}}} \tag{58}$$

This cancels for spreading pressure independent activity coefficients. In Eq. (58), the value $\psi_{1,\mathrm{lim}}$ is calculated from the definition relation of loading ψ, in the framework of the adsorbed solution theory, from the single component isotherm:

$$\psi_{1\,\mathrm{lim}} = \psi(x_1=0) = \int_0^{P_{1\,\mathrm{lim}}^*}\frac{q_1^*}{P}dp \tag{59}$$

Practical Use, Validation and Extension

The practical use of these new relations is not basically different from the RAS case. The expression of dm_t/dp_1 (Eq. (50)) can be solved for γ_1^∞ which is the only variable that is not calculable *a priori* from the single component isotherms of both components. Clearly, the same procedure is applied at the other end of the composition interval for $x_2 \to 0$, to obtain γ_2^∞. Once the γ^∞ are obtained, Eq. (54) is written twice for the limiting values:

$$\begin{aligned} RT\,\ln\gamma_1^\infty &= B(1-e^{-C\psi_{1\mathrm{lim}}}) \\ RT\,\ln\gamma_2^\infty &= B(1-e^{-C\psi_{2\mathrm{lim}}}) \end{aligned} \tag{60}$$

and this system is solved for B and C. The full description of the thermodynamic co-adsorption equilibrium is therefore achieved.

Again, the most straightforward method of testing and possibly validating this model is to recalculate the complete binary curves, using Eqs. (18) and (19) and the fitted relations for the γ_i, and to compare the weighed mass to the mass calculated using Eq. (42) for the full composition range.

An Experimental Example

This example concerns the co-adsorption of CO_2 and CH_4 on Norit RB2 activated carbon in the context of modelling hydrogen purification by PSA. The total pressure is near one atmosphere and the temperature near ambient. The corrected weight of the degassed adsorbent sample is $m_a = 0.96927$ g.

The First Step is to Measure and Exploit the Single Component Adsorption Isotherms

This was done up to 5 bars using the micro-balance in a conventional way. For measurements below one bar, the measuring cell was equilibrated with a flow of mixture of the adsorbed component with helium (the adsorption of which is negligible under these conditions), with varying partial pressure of the adsorbed component. For pressures higher than 1 bar, the cell can be equilibrated with varying total pressures of the pure adsorbed component. Measurements at partial pressures somewhat higher than what is used in the binary experiments are required for the calculation of the fictitious pressures P^* appearing in Eq. (18) and subsequently. The measured isotherms are plotted in Fig. 2, and can be represented with a good fit by a Langmuir-type isotherm with the data and parameters given in Table 1.

Table 1. Parameters of the Langmuir representation for CO_2 and CH_4 isotherms on Norit AC.at $T = 295$ K and $P = 1.011$ bar.

Temperature	Component	$1 = CO_2$	$2 = CH_4$
295 K	q_m (mol · kg^{-1})	7.94	4.87
	k (bar^{-1})	0.496	0.389
314 K	q_m (mol · kg^{-1})	6.48	4.59
	k (bar^{-1})	0.358	0.182

$$q_i = \frac{q_{im}\, k_i\, p_i}{1 + k_i\, p_i} \tag{61}$$

As shown in Appendix, the Langmuir isotherm yields analytical expressions for most of the quantities involved in the thermodynamic calculations. From these isotherms, the spreading pressure Π or more conveniently, the loading ψ for each component can be constructed by integration using Eq. (A3) in Appendix. The loading curves are shown on Fig. 3. On this figure are also indicated the graphical meaning of the limit values of $P^*(P^*_{1\,\mathrm{lim}}$ and $P^*_{2\,\mathrm{lim}})$ and of $\psi(\psi_{1\,\mathrm{lim}}$ and $\psi_{2\,\mathrm{lim}})$.

The numerical values of these quantities are obtained from Eq. (A6) and (A9). The limiting values of the adsorbed quantities q^* corresponding to the fictitious pressures P^*_{lim} and to the total pressure P are calculated from the isotherms or Eq. (A7), and finally the limit

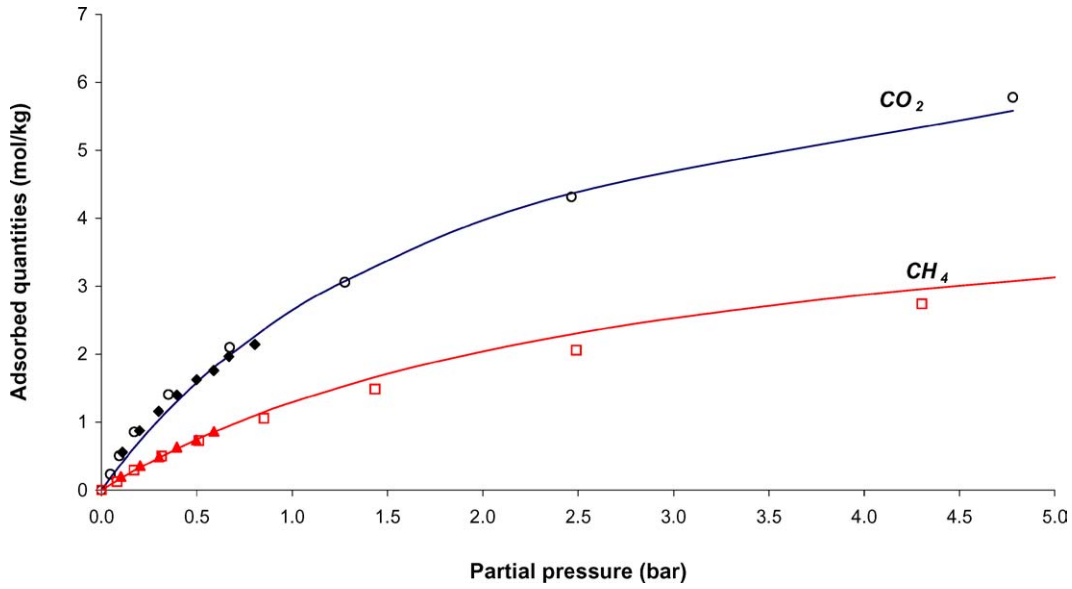

Figure 2. Adsorption isotherms of carbon dioxide and methane on Norit RB2 activated carbon at 295 K: ■, ▲: Experimental values below 1 bar obtained by the flow method, ○, □: Experimental points provided by L'Air Liquide, ——: Langmuir fit with parameters of Table 1.

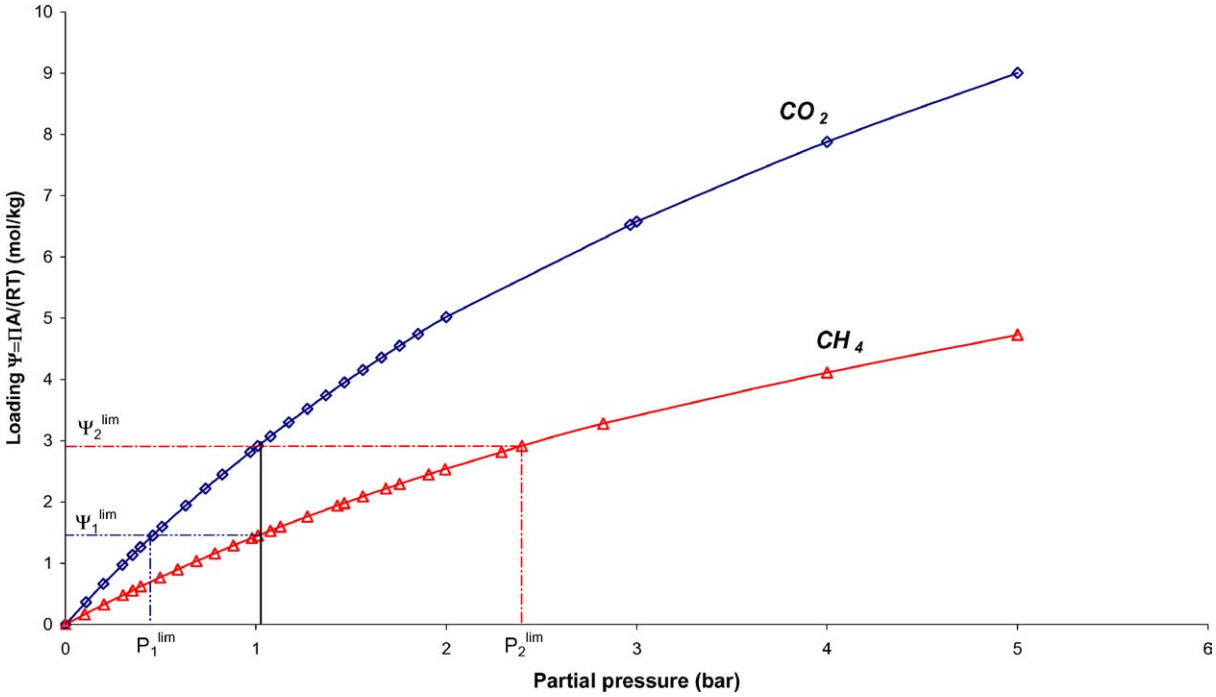

Figure 3. Loading or compressibility factor ψ versus partial pressure. The curves are obtained by integration of the isotherms using Eq. 4, and illustrate the graphical meaning of the limit values P_{lim} and ψ_{lim}.

values of the curvature parameters ξ are calculated from Eq. (16) or (A8). All the corresponding values are gathered in Table 2. Notice that so far, we have only used information from the pure component isotherms, and none from co-adsorption experiments.

In the present work, we have used the analytical approach described above, based on Langmuir isotherms. However, the binary predictions may be quite sensitive to the "quality" of the single component isotherms, and if one has very good experimental data, it may be better to use a purely numerical approach, possibly fitting the data with non-physical interpolation functions, such as splines.

Table 2. Characteristic parameters of adsorption of CO_2 and CH_4 at $T = 295$ K and $P = 1.011$ bar.

Component→	$1 = CO_2$ $(x_1 \to 0)$	$2 = CH_4$ $(x_2 \to 0)$
$\psi_{i\,\text{lim}}$ $(\text{mol}\cdot\text{kg}^{-1})$	$\psi_{1\,\text{lim}} = 1.452$	$\psi_{2\,\text{lim}} = 2.914$
P^*_{lim} (bar)	$P^*_{1\,\text{lim}} = 0.458$	$P^*_{2\,\text{lim}} = 2.397$
$q^*(P_{\text{lim}})$ $(\text{mol}\cdot\text{kg}^{-1})$	$q^*_1(P_{1\,\text{lim}}) = 1.352$	$q^*_2(P_{2\,\text{lim}}) = 2.213$
$q^*(P)$ $(\text{mol}\cdot\text{kg}^{-1})$	$q^*_1(P) = 2.491$	$q^*_2(P) = 1.270$
ξ	$\xi_{1\,\text{lim}} = 1.196$	$\xi_{2\,\text{lim}} = 1.843$

The Next Step is to Run the Perturbation Experiments and Look at the Limits

The procedure was described at the beginning of this paper. The overall result is shown on Fig. 4 for two temperatures, 295 and 314 K. The total adsorbed mass m_t, divided by the mass m_a of the "clean" adsorbent, is plotted as measured versus partial pressure of CO_2 (component 1). An interesting experimental verification is done in building the curve "from both ends", that is in our example, starting with pure CH_4 and increasing progressively the CO_2 partial pressure, and after reaching 100% CO_2, perform the reverse operation. The "upwards" and "downwards" points are distinguished on the figure, and a good consistency is observed. The total pressure in these experiments undergoes slight changes, of the order of 0.5% between the upwards and the downwards experiments. The continuous curves are a third-order polynomial fit of the overall data.

At the extremities of these curves, (limit of a small partial pressure change upon a pure component) one obtains an experimental value of dm_t/dp. This value is then compared to the value calculated using the IAS Eqs. (28) and (29), with the parameters of Table 2. This comparison is shown in Table 3 for 295 K.

Table 3. Experimental and IAS values of dm_t/dp at the composition limits (295 K).

Values of (dm_t/dp_i) $(\mathrm{g}\cdot\mathrm{bar}^{-1})$	(dm/dp_i) measured	$(dm/dp_i)^{\mathrm{IAS}}$ calc (Eq. (28))
$x_1 = x_{CO_2} \to 0$	$(dm/dp_1) = 0.14846$	$(dm/dp_1) = 0.12109$
$x_2 = x_{CH_4} \to 0$	$(dm/dp_2) = -0.08210$	$(dm/dp_2) = -0.10641$
Values of $\tilde{M}$ (Eq. (29)) $(\mathrm{kg}\cdot\mathrm{mol}^{-1})$	$\tilde{M}_1 = 0.1216$	$\tilde{M}_2 = -0.0011$

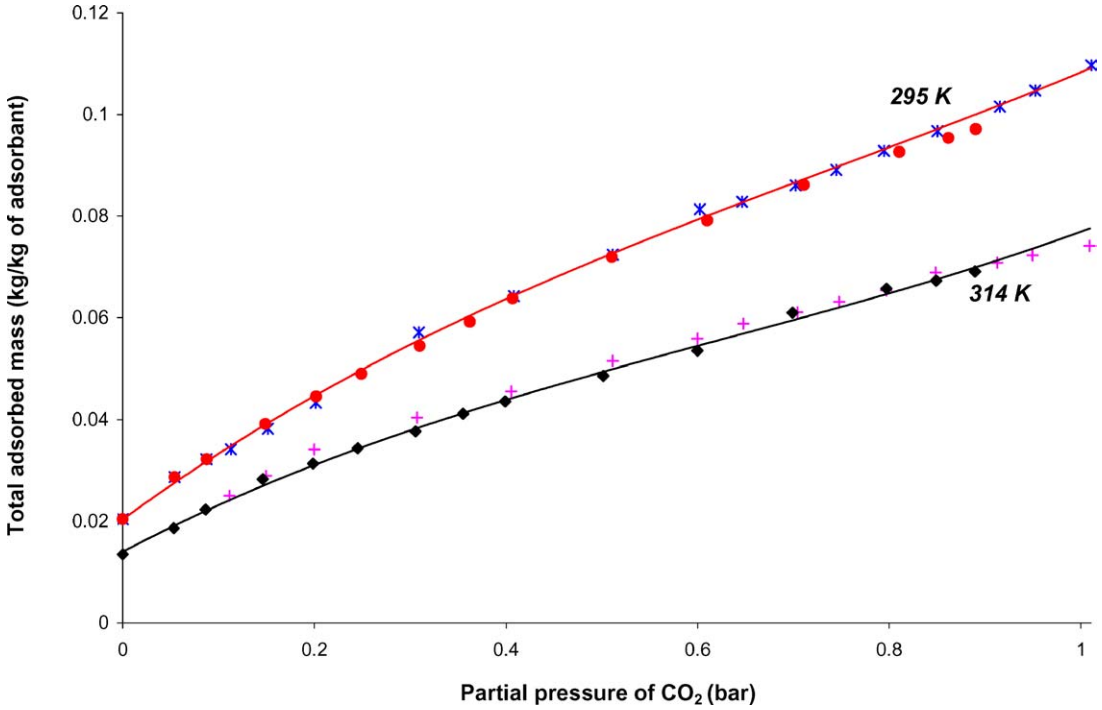

Figure 4. Total adsorbed mass ratio versus partial pressure at two temperatures. The ordinate is m_t/m_a, i.e. the value measured by the microbalance minus the mass of the clean adsorbent, divided by the mass of adsorbent ($m_a = 0.96927$ g). $*, +$: Experimental values at *decreasing* CO_2 concentration, ●, ♦: Experimental values at *increasing* CO_2 concentration, —— Cubic polynomial fit.

It can be observed that the measured and calculated values are in the "good" order of magnitude and sign, but we can certainly expect a better fit with a more elaborate model.

Next, the Full Equilibrium is Calculated Using the IAS Algorithm

A convenient algorithm for the IAS calculations is the following:

– pick a series of values of ψ between $\psi_{1\,\mathrm{lim}}$ and $\psi_{2\,\mathrm{lim}}$ of Table 2
– for each Ψ compute P_1^* from Eq. (A3) or (A4)
– obtain the solid phase composition x_i from:

$$x_1 = (P_2^* - P)/(P_2^* - P_1^*) \quad x_2 = 1 - x_1$$

– obtain $q_1^*(P_1^*)$ and $q_2^*(P_2^*)$ from the isotherms
– compute the total adsorbed quantity q_t from Eq. (19) without the second term
– obtain the individual adsorbed quantities q_i as $q_t \cdot x_i$
– obtain the gas phase composition y_i from Eq. (18) as $x_i \cdot P_i^*/P$

Figure 5 shows the plot of these calculated binary isotherms, where the adsorbed quantities are expressed in mass and referred to a unit mass of adsorbent. The IAS-predicted curve of the total adsorbed mass can now be compared to the experimental result. A significant

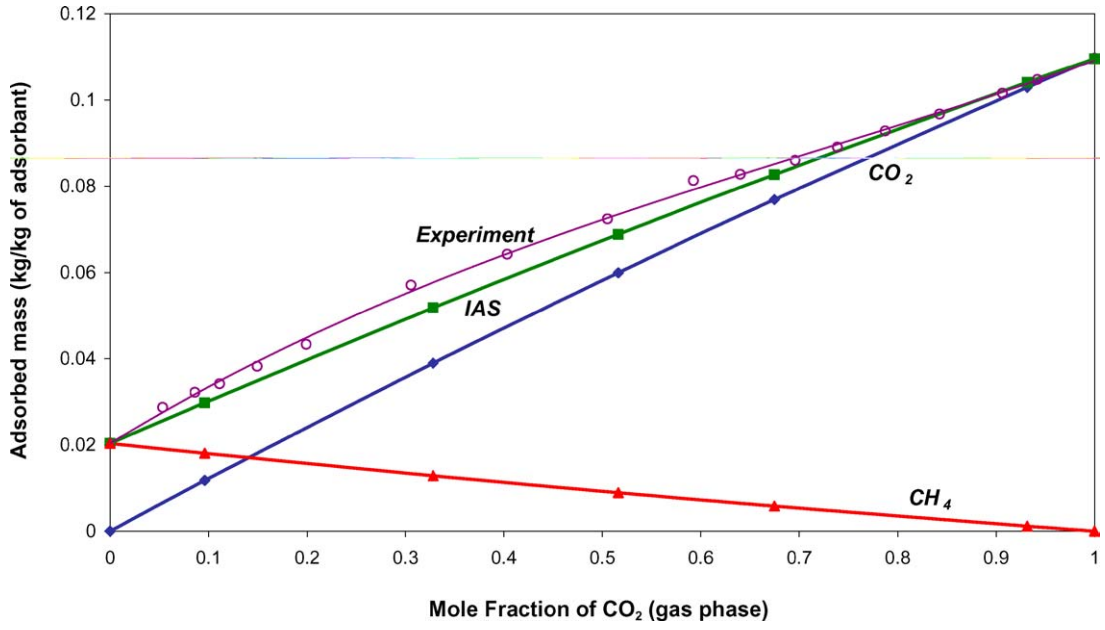

Figure 5. Binary isotherms at 295° K and 1.01 bar. IAS predictions and experiment. ○: Total adsorbed mass ratio measured (identical to that of Fig. 4). ■: Total adsorbed mass ratio calculated by the Ideal Adsorbed Solution (IAS) model. ♦, ▲: Individual component adsorbed mass ratio calculated by the IAS model. ——: Graphical fit.

difference is observed which may justify a more elaborate model.

The Limiting Activity Coefficients are then Determined

The measured values of dm_t/dp (Table 3) can be used to evaluate limiting activity coefficients, using Eq. (40). The results are in Table 4 and we observe that the values of γ^∞ are smaller than 1.

Models for Non-Ideal Solutions are Tested

We can now implement some classical model for activity coefficients. Five models involving two adjustable parameters have been tested here: Wilson, Van Laar, Margules, Flory-Huggins, and ISAC. The first four are presented and can be found in most chemical thermodynamics books (for example Sandler, 1999). For ISAC, one has to refer to the original publication by Kopatsis et al. (1988). They all derive from a form of the Gibbs excess energy and satisfy the Gibbs-Duhem constraint. The Van Laar model corresponds to the Regular Solution assumptions, including a zero excess entropy of mixing. The Wilson, Margules and Flory-Huggins models are used with the RAS assumption of zero excess surface of mixing, i.e. without the last term in Eq. (19).

The ISAC model contains an explicit dependence of Gibbs energy and of activity coefficients on loading (SPD framework), and therefore accounts for this term in Eq. (19). Table 5 gathers the constitutive equations of these five models. Using the values of γ^∞ thus determined and the limiting equations for Ln γ^∞, the unknown parameters are determined directly for the Van Laar and the Margules equations. For the Wilson, ISAC and Flory-Huggins models, the couple of nonlinear equations can be reduced to a single equation which needs to be solved by a numerical search, but which has seemingly *a unique physical solution*. The values of the parameters of the five models are given in Table 6, and Fig. 6(a) and (b) are a representation of the

Table 4. Calculation of infinite dilution activity coefficients in adsorbed phase from the measured limit values of dm_t/dp.

Infinite dilution activity coefficients	CO_2 $x_1 = x_{CO_2} \to 0$	CH_4 $x_2 = x_{CH_4} \to 0$
Coefficient Q (Eq. (41))	0.0359	0.1256
Coefficient R (Eq. (41))	0.1970	0.0192
γ^∞ (Eq. (40))	$\gamma_1^\infty = 0.8515$	$\gamma_2^\infty = 0.4417$
Ln γ^∞	−0.16075	−0.81712

Table 5. Characteristics of the five non-ideal solutions models tested.

	Margules	*Wilson*	*ISAC*	*Flory-Huggins*	*Van Laar*
G^{ex}	$x_1x_2[A+B(x_1-x_2)]$	$RT^*[-x_1\cdot\ln(x_1+\Lambda_{12}\cdot x_2)-x_2\cdot\ln(x_2+\Lambda_{21}\cdot x_1)]$	$\frac{B}{RT}x_1x_2(1-e^{-C\psi})$	$x_1\cdot\ln\frac{\varphi_1}{x_1}+x_2\cdot\ln\frac{\varphi_2}{x_2}+\chi\cdot(x_1+m\cdot x_2)\cdot\varphi_1\cdot\varphi_2$	$RT^*\left[\frac{2Ax_1x_2q_1q_2}{x_1q_1+x_2q_2}\right]$
$ln\ \gamma_1$	$\alpha_1x_2^2+\beta_1x_2^3$	$-\ln(x_1+\Lambda_{12}\cdot x_2)+x_2\left(\frac{\Lambda_{12}}{x_1+\Lambda_{12}x_2}-\frac{\Lambda_{21}}{x_2+\Lambda_{21}x_1}\right)$	$\frac{B}{RT}x_2^2(1-e^{-C\psi})$	$\ln\frac{\varphi_1}{x_1}+\left(1-\frac{1}{m}\right)\cdot\varphi_2+\chi\cdot\varphi_2^2$	$\frac{\alpha}{\left[1+\frac{\alpha}{\beta}\frac{x_1}{x_2}\right]^2}$
$ln\ \gamma_2$	$\alpha_2x_1^2+\beta_2x_1^3$	$-\ln(x_2+\Lambda_{21}\cdot x_1)+x_1\left(\frac{\Lambda_{21}}{x_2+\Lambda_{21}x_1}-\frac{\Lambda_{12}}{x_1+\Lambda_{12}x_2}\right)$	$\frac{B}{RT}x_1^2(1-e^{-C\psi})$	$\ln\frac{\varphi_2}{x_2}-(m-1)\cdot\varphi_1+\chi\cdot\varphi_1^2$	$\frac{\beta}{\left[1+\frac{\beta}{\alpha}\frac{x_2}{x_1}\right]^2}$
$ln\ \gamma_1^\infty$	$\alpha_1+\beta_1=A-B$	$1-\ln\Lambda_{12}-\Lambda_{21}$	$\frac{B}{RT}\left(1-e^{-C\psi_1^{\lim}}\right)$	$-\ln(m)+\left(1-\frac{1}{m}\right)\cdot+\chi$	α
$ln\ \gamma_2^\infty$	$\alpha_2+\beta_2=A+B$	$1-\ln\Lambda_{21}-\Lambda_{12}$	$\frac{B}{RT}\left(1-e^{-C\psi_2^{\lim}}\right)$	$\ln(m)-(m-1)+\chi$	β
	$\alpha_1=A+3B;\alpha_2=A-3B$			$\varphi_1=x_1/(x_1+m\cdot x_2)$	$\alpha=2Aq_1$
	$\beta_1=-\beta_2=-4B$			$\varphi_2=m\cdot x_2/(x_1+m\cdot x_2)$	$\beta=2Aq_2$

Table 6. Numerical values of model parameters for activity coefficients $CO_2 + CH_4$ on Norit AC at 295 K.

Wilson	Van Laar	Flory-Huggins	Margules	ISAC
			$\alpha_1 = -1.4733$	
$\Lambda_{12} = 0.00708$	$\alpha = -0.1608$	$m = 3.396$	$\beta_1 = 1.3125$	$B/RT = 0.05310$
$\Lambda_{21} = 6.11111$	$\beta = -0.8170$	$\chi = 0.3563$	$\alpha_2 = 0.4955$	
			$\beta_2 = -1.3125$	$C = -0.95951$

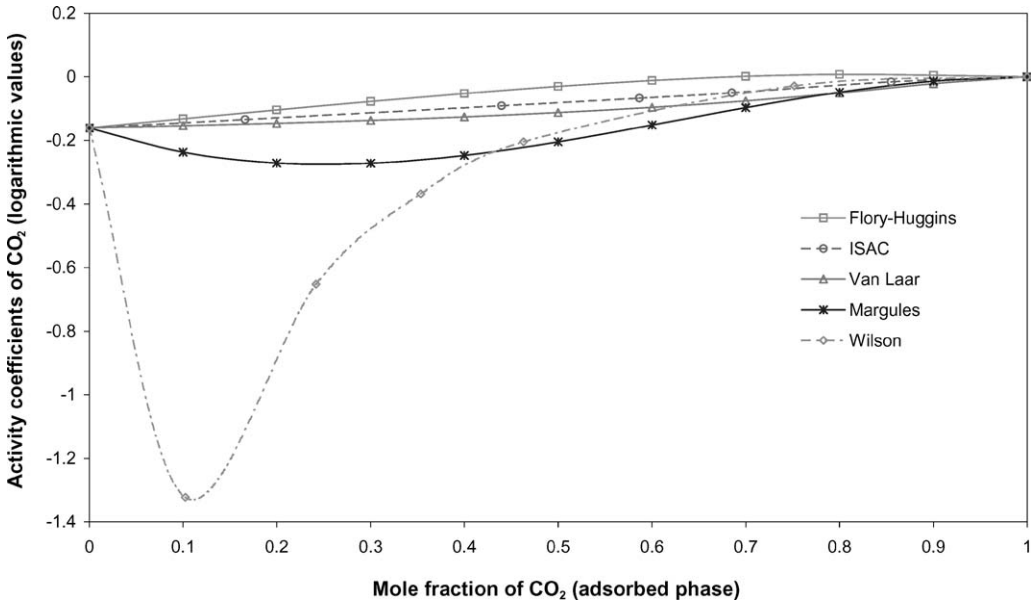

(a)

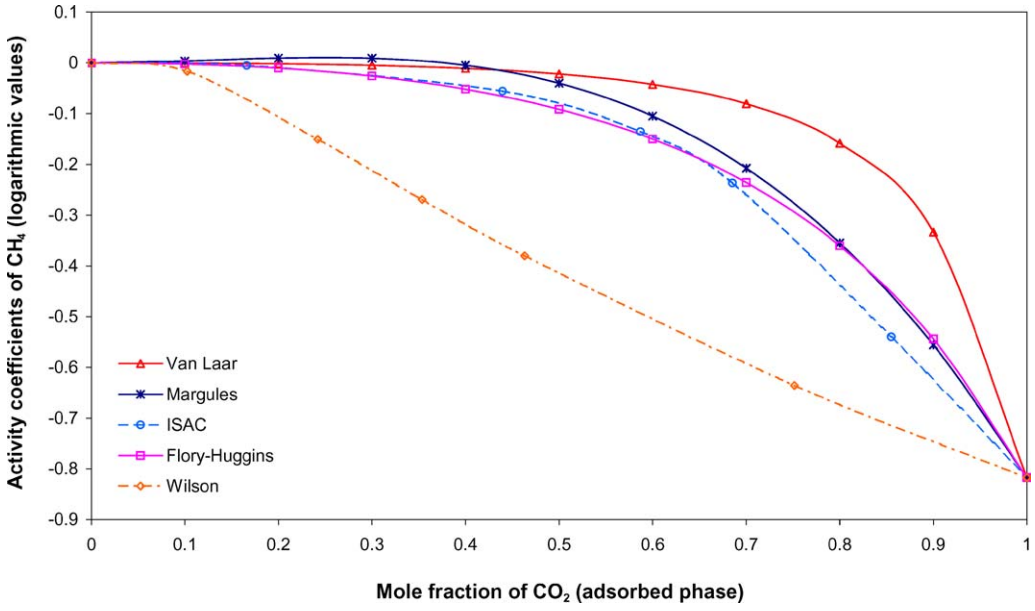

(b)

Figure 6. Variation of activity coefficients with binary composition for five models (295 K; 1.01 bar). 6a: CO_2 6b: CH_4.

Table 7. Deviation of models from experiment for the total adsorbed mass (295 K).

Model→	IAS	Wilson	Van Laar	Flory-H.	Margules	ISAC
Deviation%						
Standard deviation	13.21	5.15	2.15	3.86	0.79	2.91
Mean deviation	11.52	3.33	1.80	3.24	0.68	2.24

variation of the activity coefficients with composition. It is seen that the variation of the γ is qualitatively similar except for the Wilson model, and this will have a significant influence on the isotherms themselves. Notice that Lnγ is essentially negative ($\gamma < 1$) for all models and over the whole range (negative deviation from Raoult's law) except a very slightly positive zone for CH_4 with Margules, and a practically zero zone for CO_2 with Flory-Huggins. Of course, all models satisfy the conditions that when the mole fraction of a component tends to 1, the logarithm of its activity coefficient tends to 0 with zero slope, as required by the Gibbs-Duhem constraint.

The Flory-Huggins model has a particular status here, since it is not a regular solution model (the excess entropy is non-zero). It is actually the only model that does not satisfy Herington's consistency test (Herington, 1947):

$$\int_0^1 \ln\left(\frac{\gamma_1}{\gamma_2}\right) dx = 0 \quad (\text{const } T \text{ and } \psi) \tag{62}$$

We believe that this is due to an improper use of this model (imposing the assumption of zero excess area) and not to an intrinsic inconsistency. In addition, the value of the parameter m, given in Table 6, has visibly no relation with the ratio of molar volumes of the two components, as the physical interpretation of this model implies. On the other hand, it could be interpreted more realistically as space, or number of sites, occupied by the adsorbed molecules on the adsorbent surface. The reason for testing this model is its relation to sorption in polymers, and thus possibly to adsorption, but its use here should be considered as purely empirical.

The Full Equilibrium is Now Computed with These Different Models

This implies solving the RAS equations, that is Eq. (18) with the activity coefficients, and Eq. (19) (without the spreading pressure dependent term for the first four models, with this term for the ISAC model). The algorithm is not basically different from that presented above in Section 3, except that the calculation of the adsorbed phase composition is not explicit, and requires a simple numerical search.

A first interesting and useful test is to compare the total adsorbed mass curves for the different models with the experimental results. This is done on Figs. 7(a) and (b) for two temperatures, 295 K and 314 K. The data and parameters for this second temperature are gathered below in Table 9 and will be discussed later. It is seen that at 295 K, all models give visually "correct" results, with an underestimation for IAS, a better fit for Margules and a relatively poorer one for Wilson in the low CO_2 region. The picture is quite different at 314 K, where none of the models gives really excellent results. Margules is again the best choice. Table 7 gives quantitative measures of the standard deviation and the arithmetic average deviation of the models with experiment, and confirms the visual impression.

Figure 7(c) illustrates a peculiarity of the present method which we want to emphasize. It is a plot of the same results as Fig. 7(a), at 295 K, but using the more usual mole concentration in the adsorbed phase, instead of the mass concentration. The problem of this representation is that it is not a direct representation of the experimental result, since the adsorbed phase composition has to be calculated using one of the models (in the case of Fig. 7(c), with used the Margules relation). Therefore, the validation and comparison with experiment should be done exclusively with plots such as Figs. 7(a) and (b).

Figures 8(a) and (b) show the reconstitution of the individual adsorption curves for the two components, at the two temperatures, using the Margules model. Obviously, similar diagrams are easily generated with the other models, but the only evaluation criterion that we have is the total adsorbed mass, as shown above. It may be tempting to conclude that the Margules model is the best choice in general, owing to its simplicity and to the good present results. There are no theoretical grounds for such a general conclusion though.

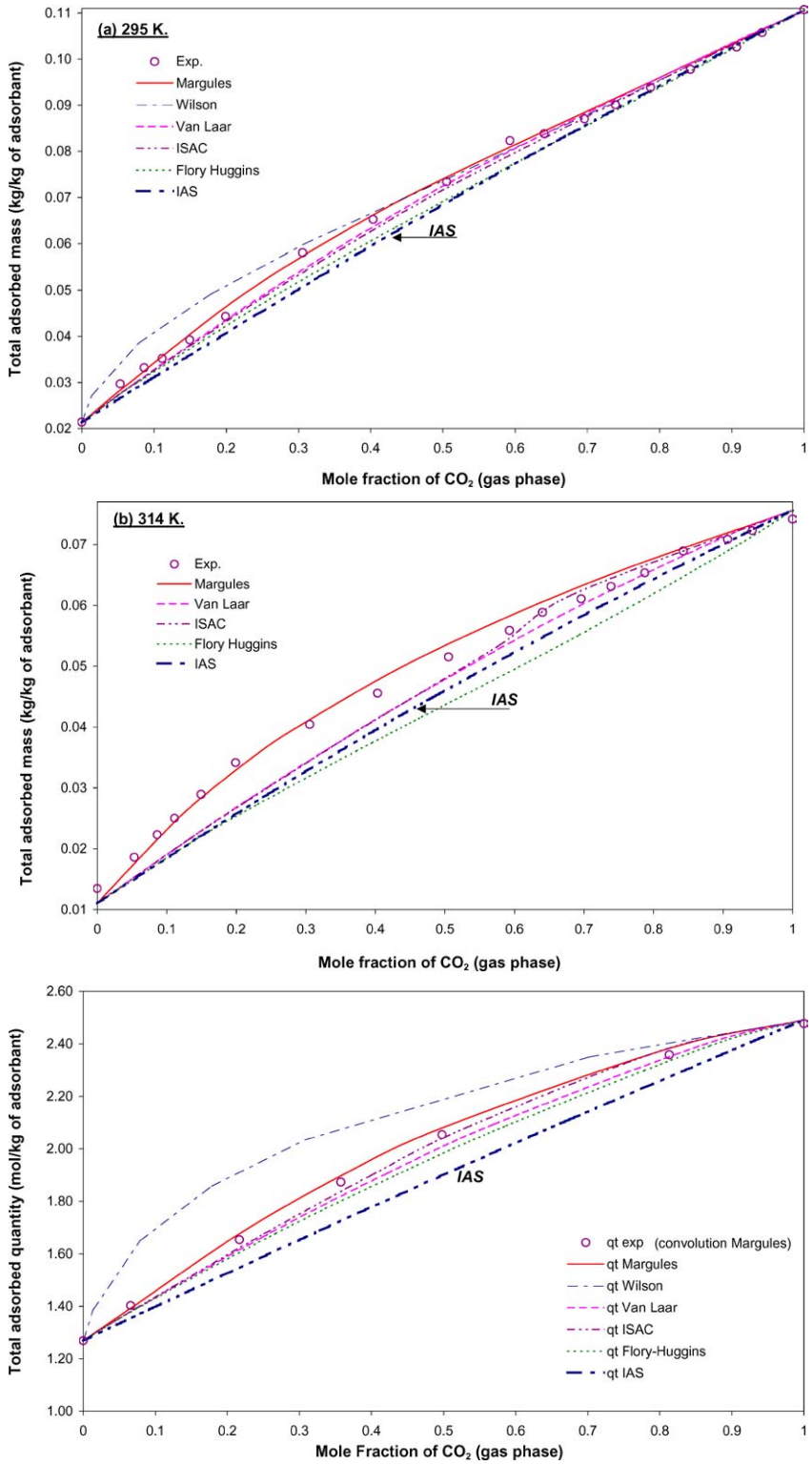

Figure 7. Comparison of the experimental total adsorbed mass ratio with the predictions of the ideal (IAS) model and with the five non-ideal models. 7(a): 295 K; 7(b): 314 K; 7(c): Mole concentration in the adsorbed phase, 295 K.

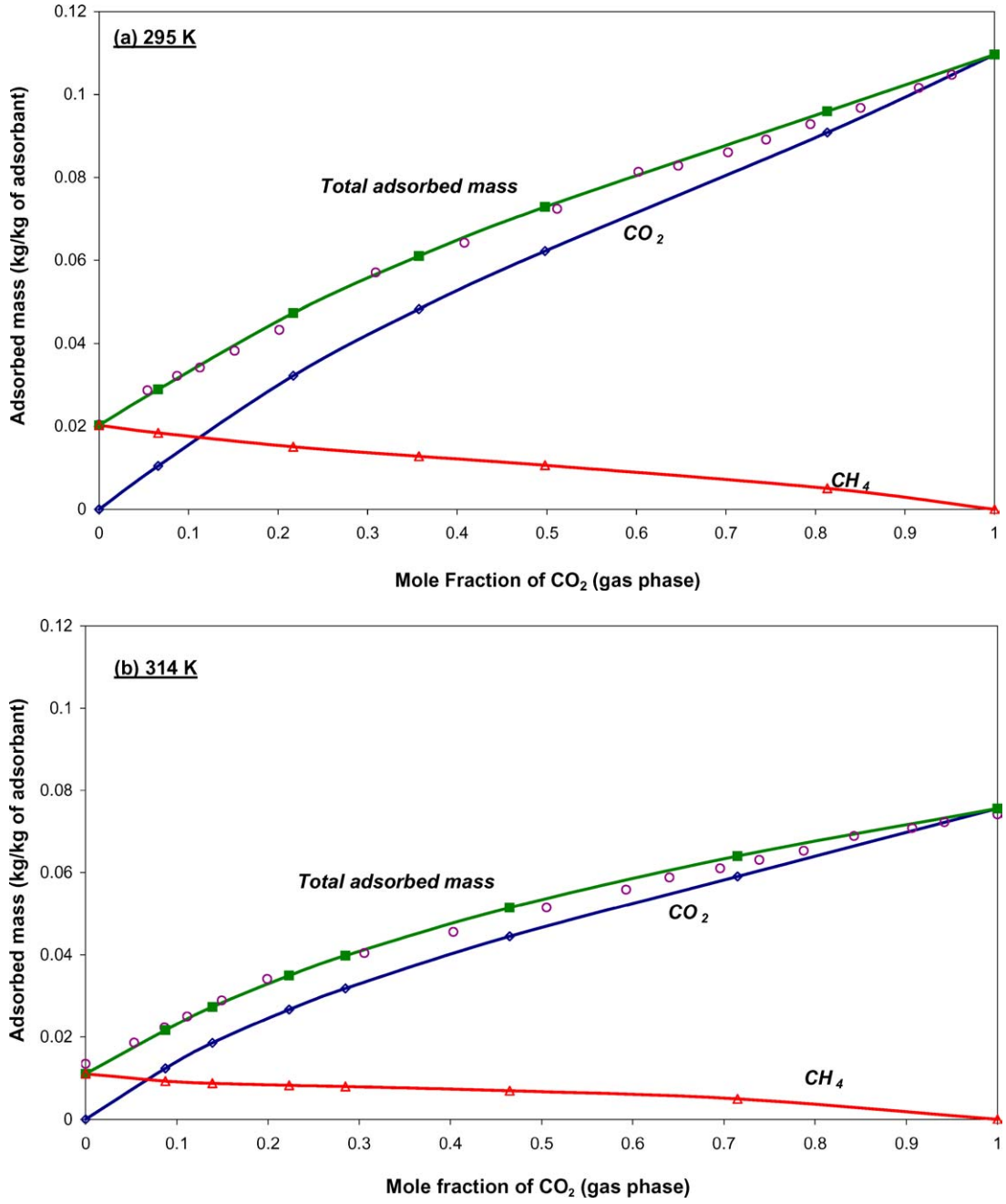

Figure 8. Binary adsorption isotherms described by the two-parameter Margules model. The Margules model is in Table 5 and the parameter values are in Table 6. 8(a): 295 K; 8(b): 314 K. ○: Total adsorbed mass ratio, experimental values; ■: Total adsorbed mass ratio, calculated; ◇, Δ Individual components, calculated; ——: graphical fit.

A further representation of the full equilibrium is the "phase diagram", where the adsorbed phase composition x is plotted versus the gas phase composition y at equilibrium. Figure 9 shows this diagram as constructed with the different models at 295 K, and indicates that this representation has little sensitivity to the choice of the model. The differences are emphasised and the relative position of the curves appears more

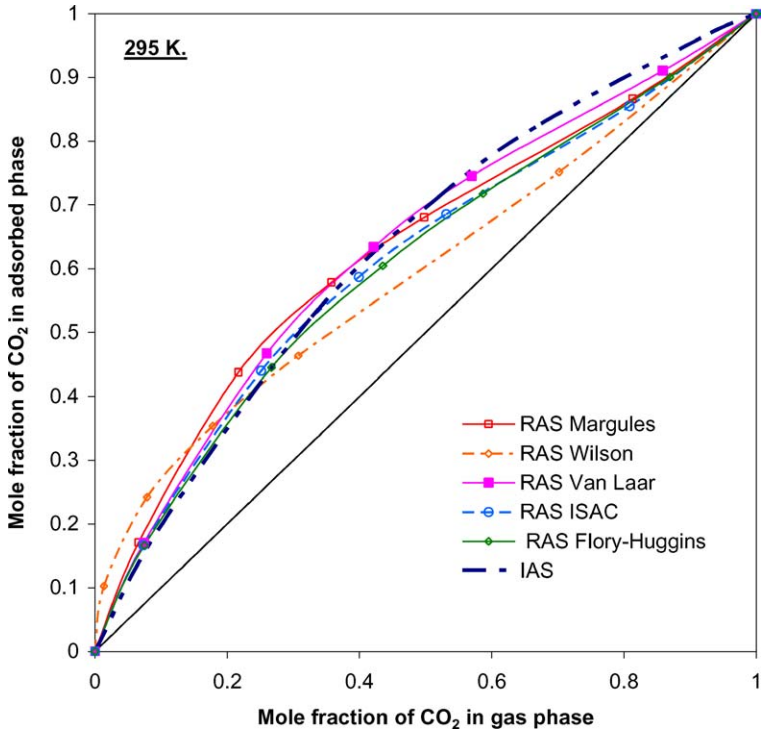

Figure 9. Phase diagram for CO_2 calculated from experimental data using different models.

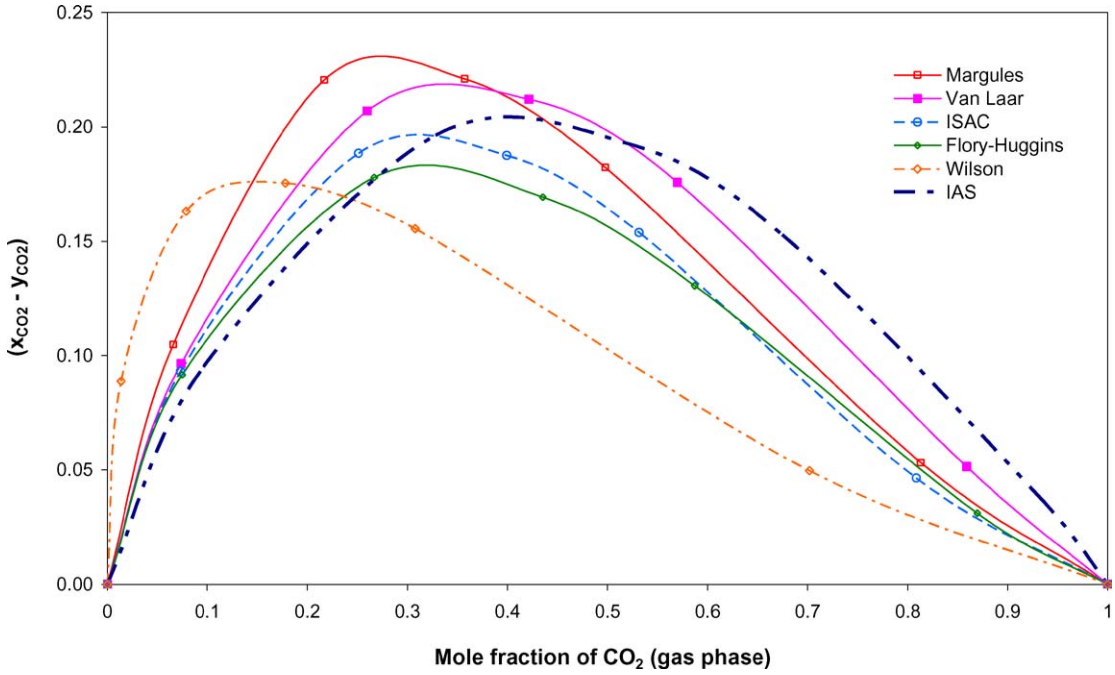

Figure 10. Difference phase diagram calculated from different models at 295 K. The ordinate represents the difference between the adsorbed mole fraction x predicted from the models and the gas phase mole fraction y.

clearly when one plots as ordinate the difference $x - y$, in other words, the vertical distance of the curve from the diagonal, as in Fig. 10.

Discussion and Extensions

Validation with Independent Data

It is of interest to test the complete approach using "complete" data, that is where the adsorbed quantities of each component is measured, not just the total adsorbed mass. For this purpose, we have used co-adsorption data furnished by L'Air Liquide for a total pressure of 2.06 bars and 293 K. The adsorbed concentrations were determined using a material balance on a batch equilibration technique with measurement of the gas phase composition at equilibrium, and the total adsorbed quantity curve is obtained by their summation. These experimental data appear as discrete points in Fig. 11. The curve of total adsorbed mass is then smoothed with a polynomial to evaluate the limiting slopes dm/dp. We then recalculated the characteristic parameters at this new total pressure from the single component isotherms of Fig. 2, neglecting the temperature difference between 293 and 295 K, and the infinite dilution activity coefficients are determined as in the experimental example above, using only the limiting slopes of the smoothed total adsorbed mass curve. Table 8 summarizes the numerical results.

Table 8. Data and parameters for the CO_2-CH_4 isotherm at 293 K, $P = 2.06$ bar.

i	$1 = CO_2$	$2 = CH_4$	Units
ψ_{lim}	2.598	5.122	$\text{mol} \cdot \text{kg}^{-1}$
P_{lim}	0.884	5.578	bar
$q_{\text{lim}}(P)$	3.862	2.031	$\text{mol} \cdot \text{kg}^{-1}$
$q_{\text{lim}}(P_{\text{lim}})$	2.263	3.205	$\text{mol} \cdot \text{kg}^{-1}$
ξ_{lim}	1.377	1.092	–
$(dm/dp_i)_{xi=0}$	0.1058	−0.0490	$\text{g} \cdot \text{bar}^{-1}$
Q_i	0.0167	0.1069	$\text{g} \cdot \text{bar}^{-1}$
R_i	0.1049	0.0158	$\text{g} \cdot \text{bar}^{-1}$
γ_i^{∞}	0.856	0.273	–

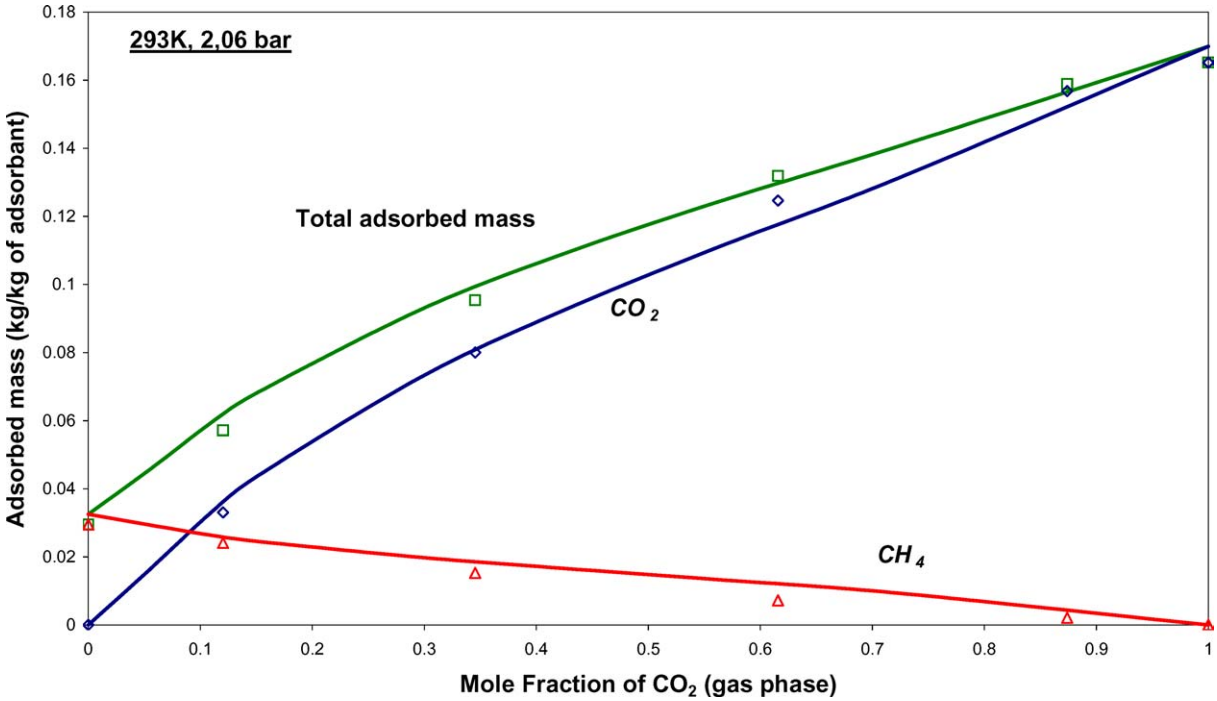

Figure 11. Binary isotherms at 293 K and 2.06 bar, predicted and experimental. △, ◇: Measured mass concentrations of individual components, □: Total mass adsorbed calculated as the sum of the individual components, ——: Calculated curve using the single component isotherms of Fig. 2 and the Margules model with the parameters at 2.06 bar (Table 8).

These activity coefficients were then used with the Margules model to construct the binary co-adsorption isotherms shown as continuous lines on Fig. 11. The standard deviation on the total adsorbed mass is about 3%, while it is of the order of 7% for CO_2 and 15% for CH_4. The procedure over-predicts CH_4 adsorption and under-predicts CO_2 adsorption. It is noteworthy that the value of γ_1^∞ is almost the same as at 1 bar, and that the results are rather sensitive to this value, while they are relatively insensitive to the value of γ_2^∞, which is very different from that at 1 bar.

Model Dependence and Number of Parameters

The approach presented here starts with the determination of γ_1^∞ and γ_2^∞. The values found are "mathematically univocal", meaning that there is only one set of values satisfying the equations that determine them, given the measured quantities. Within the RAS approach, the values found are also model-independent, i.e. they are the same for Wilson, Van Laar, Margules or any other spreading pressure independent model for composition dependence. In addition, the two parameters of the models used here are also uniquely determined. They account for the full composition dependence of the activity coefficients.

In the SPD approach on the other hand, the values of γ_1^∞ and γ_2^∞ depend on the spreading pressure dependence postulated, for instance, that of ISAC, and in that sense are model-dependent. This dependence requires the introduction of at least one parameter, so that only one parameter is left to account for the composition dependence. The question posed is then how to handle models with more parameters, for example combining a two-parameter Margules or Wilson expression for the composition dependence with the exponential factor of the ISAC model. This was done for example in the paper by Myers (1989), by an optimization method of the three parameters, using binary data *at different pressures*. A similar approach could in principle be taken here using all the experimental data available *at one pressure*, not just the limiting γ's. As an initial guess, one may use the infinite dilution γ values estimated as for RAS. But the "one pressure" fitting approach does not discriminate between the effect of the spreading pressure and the effect of composition on the activity coefficients, and is therefore a relatively blind fitting that does not guarantee coherence. We discuss this question further in connection with the pressure dependence of activity coefficients.

Pressure Dependence of Activity Coefficients and Prediction at other Pressures

As suggested by Van der Vaart et al. (2000), it would seem a priori reasonable to *assume* that the activity coefficients are independent of total pressure, an assumption coherent with the picture of the Regular Adsorbed Solution Theory. To substantiate this assumption, one may notice that the Helmholtz energy of condensed phases is practically pressure independent and if the excess surface of mixing is assumed zero, the Gibbs excess energy is equal to the Helmholtz excess energy. This does not strictly imply independence with respect to spreading pressure, but probably a weak dependence. A possible application of this approach would then be to predict the co-adsorption of the same constituents under different pressures. We have thus tried to represent the binary system at 2.06 bar using the activity coefficients at 1 bar. The resulting curves give a representation (not shown here) that is only slightly poorer than that of Fig. 11, with the same trends (good fit for the total mass, over-prediction of CH_4 adsorption and under-prediction of CO_2 adsorption). The pressure independence of the activity coefficients may thus be taken as an approximation.

Let us now compare the values obtained above at 1.01 bar (Table 4) and at 2.06 bar (Table 8). It is seen that $\gamma^\infty(x_{CO_2} = 0)$ practically has the same value, and can thus be considered pressure independent. Such is not the case for $\gamma^\infty(x_{CH_4} = 0)$, which is almost divided by two when doubling the pressure. This trend has a low sensitivity to the value of dm/dp, and is mostly sensitive to the properties of the single component isotherms. It is clear that for accurate values of the infinite dilution activity coefficient, pressure independence is not acceptable, even though, as mentioned above, the binary curves are relatively insensitive to γ_2^∞.

For a more accurate prediction of the binary curves, changing the limiting activity coefficient with pressure is apparently not sufficient. What is actually missing here is a detailed description of the spreading pressure dependence. In a forthcoming publication, we shall show how a complete 4-parameter SPD model can be built univocally, using data at two pressures, without recourse to a fitting method. The methodology and the calculations are too long to be presented in the present paper.

Table 9. Data and parameters for the CO_2-CH_4 isotherm at 314°K, $P = 1.01$ bar.

i	$1 = CO_2$	$2 = CH_4$	Units
q_m^*	6.48	4.59	$mol \cdot kg^{-1}$
b_i	0.358	0.182	bar^{-1}
ψ_{lim}	0.737	1.967	$mol \cdot kg^{-1}$
P_{lim}	0.347	3.123	bar
$q_{lim}(P)$	1.718	0.690	$mol \cdot kg^{-1}$
$q_{lim}(P_{lim})$	0.706	1.624	$mol \cdot kg^{-1}$
ξ_{lim}	1.141	1.539	–
$(dm/dp_i)_{xi=0}$	0.0929	−0.0312	$g \cdot bar^{-1}$
Q_i	0.0163	0.0827	$g \cdot bar^{-1}$
R_i	0.1020	0.0105	$g \cdot bar^{-1}$
γ_i^∞	0.9346	0.2034	–
$\bar{h}_i^{ex}$	−3.39	+28.23	$kJ \cdot mol^{-1}$

Temperature Dependence of Activity Coefficients

As for temperature, there is no reason to expect any simple dependence, and clearly new single component isotherms have to be measured as well as new activity coefficients. We have made measurements of the total adsorbed mass at 314 K and 1.01 bar (Fig. 4) and determined the corresponding activity coefficients. Table 9 gives the corresponding parameters and activity coefficients, Fig. 7(b) shows the representation of the total adsorbed mass, and Fig. 8(b) shows the binary isotherms.

By comparing with Table 4, we clearly see a strong dependence of the infinite dilution activity coefficients on temperature, with an increase with temperature for CO_2 and a decrease for CH_4. The data at different temperatures can be used to evaluate thermodynamic quantities that are essentially excess partial molar enthalpies, and may be assimilated to activation energies for the activity coefficients:

$$\left(\frac{\partial \ln \gamma_i}{\partial T}\right)_{P,x} = \frac{\partial}{\partial T}\left(\frac{\overline{g}_i^{ex}}{RT}\right)_{P,x} = -\frac{\bar{h}_i^{ex}}{RT^2} \qquad (63)$$

Assuming either that $\bar{h}_i^{ex}$ is a constant or that the temperature interval is small, this equation may be integrated into:

$$\ln \gamma_i(T_2) - \ln \gamma_i(T_1) = \frac{\bar{h}_i^{ex}}{R}\left[\frac{1}{T_2} - \frac{1}{T_1}\right] \qquad (64)$$

The measured values of γ_i^∞ may be used to evaluate $\bar{h}_i^{ex}$. Their order of magnitude is given in Table 9. When assumed constant in a range, they can be used for interpolation or moderate extrapolation.

Comparison with Earlier Data

As mentioned in the introduction, a few earlier studies concern co-adsorption of carbon dioxide and methane on activated carbon, and its description using activity coefficients. The data of Buss (1995) show activity coefficients larger than unity over the whole composition range, for an activated carbon with large pores and a relatively homogeneous surface. The data of Van der Vaart et al. (2000) on Norit RB1 should be more in agreement with the present findings, since the isotherms for the pure components at 1 bar, the total mass adsorbed and the co-adsorbed concentrations of CO_2 are quite close to that found here. Nevertheless, the activity coefficients are significantly different. The Wilson parameters as fitted by these authors are $\Lambda_{12} = 2.8$ and $\Lambda_{21} = 0.018$ (to compare to our values $\Lambda_{12} = 0.0071$; $\Lambda_{21} = 6.1111$) corresponding to $\gamma_1^\infty = 0.954$ and $\gamma_2^\infty = 9.18$. In particular, the large value of the activity coefficient for CH_4 contradicts our small value of 0.442.

We are tempted to explain this difference by the fact that the limiting activity coefficients do not enter at all in the Van der Vaart calculations, and that their Wilson fit is somewhat rough, whereas they are the fundamental data in our approach, and their values entirely determine the shapes of the Wilson plot. The qualitative difference is that in our case, the activity is practically always smaller than that of an ideal bulk mixture, whereas the Van der Vaart values shows a very high activity of methane at low concentrations. These features should probably be explained on physical grounds.

Conclusion

Let us discuss critically the methodology proposed in the light of the examples and results presented.

Experimental Simplicity, Practical Convenience, Theoretical Complexity. The main interest of this approach is its experimental simplicity. Besides the single component isotherms, only two measurements are strictly necessary, at the limits of large dilution, to obtain the two basic parameters, the γ^∞. But such measurements are rather difficult and on the other hand, the complete gravimetric curve is convenient to

obtain. The latter is thus used for testing the experimental conditions (incremental and decremental curves should coincide), for extrapolation to infinite dilution, as a verification of the overall fit of the model, and also to discriminate between activity models. Choosing *a priori* a simple model for the activity coefficients, such as Margules or Van Laar, suffices to construct a reasonable estimate of the complete binary isotherm. The theoretical complexity has to be faced only once: once the formulae are established, the calculations and algorithms are quite straightforward.

Model Versus Measure. Let us first recall that the approach proposed aims at building a thermodynamic model of the equilibria capable of representation, of extrapolation, of multi-component extension, and of incorporation in a process simulator. Model building includes parameter determination and model discrimination. Measuring the total mass adsorbed in the binary system (together with the single component isotherms) gives sufficient information for this purpose, under certain assumptions. It is not an information equivalent to measuring the individual adsorbed quantities, and this approach should not be considered as an alternative to full measuring techniques.

Thermodynamic Assumptions, Accuracy, Versatility and Coherence. The versatility and fitting power of the models used here are restricted by two factors:

- the fact that two adjusted parameters only are introduced, and that we want them uniquely determined by the measured data;
- the fact that the models are thermodynamically coherent, in the sense of satisfying all thermodynamic constraints coherent with the assumptions (such as Gibbs-Duhem), and the assumptions themselves are not thermodynamically prohibited.

These factors contribute to convenience of use and to predictive power, which in a sense we pay for in loss of versatility and fitting power. If more accuracy and more versatility are sought, more parameters are needed. Unicity of these parameters and thermodynamic coherence can only be preserved if more measured data are used in the framework of an extended model. We shall show how this can de done in a forthcoming paper.

Unicity of the γ^∞ and Model Dependence. The fact that we get the γ^∞ from one experimental information only at each end of the composition range stems from the thermodynamic constraints and from choosing a two parameter model. Any additional measurement is redundant and must be reconciliated with the above. The analytical and linear character of the expressions for the γ^∞ (Eqs. (40)–(41) or (50)–(51)) ensures that the solutions for the γ^∞ corresponding to given experimental data are unique (contrarily to any global fitting method). As mentioned above, they are also model-independent for the RAS models, but not for the SPD models.

The different models for the composition dependence of the γ can be discriminated only through a numerical best fit criterion, using for example the full adsorbed mass curve, not through a thermodynamic criterion. The model of activity coefficient variation is therefore not unique. Other models are available than those used here. For example the UNIQUAC approach (Abrams and Prausnitz, 1975) also involves two parameters that can be determined in this way, but together with a number of chemical parameters obtained from tables. The Non-Random Two-Liquids model (Renon and Prausnitz, 1968) involves 3 parameters, and would require a global fitting approach.

Just as the Adsorbed Solution Theory, the approach proposed is in principle independent of the model chosen to represent the single-component isotherms. In our specific example, we have used Langmuir isotherms because they turn out to represent reasonably our data, and in addition, are convenient for calculations (see Appendix). But any other model fitting well the isotherm data would do, and as a matter of fact, no explicit model at all is needed. Since the quality of the binary representation is sensitive to the quality of the single component representation, if accurate experimental data are available, it may be better to use a table of measured values with a suitable interpolation rule rather than an analytical model.

Extensions and Perspectives. A number of open questions and of potential developments are left for future work, concerning the experimental procedure as well as the theory. Among these, we should like to mention: use of temperature programming to obtain conveniently temperature dependent data; interpolation between different pressures and temperatures, as envisaged through Eq. (63); obtain binary data at different total pressures using an inert gas; generate approximate but consistent analytical expressions for the co-adsorption curves; extend the approach to

heterogeneous surfaces; incorporate the binary co-adsorption results into a general model of multi-component column operation.

But the main point seems the need to extend the approach to models accounting for spreading pressure dependence and with more parameters, as suggested by Myers' work (Myers, 1989). Besides being more in coherence with the full non-ideal adsorbed solution theory, one would certainly gain in both fitting power and predictive power. While this paper was being reviewed, we have actually set the bases for such a development, introducing two additional parameters, obtained independently from data at two different pressures. This will be presented in a forthcoming paper.

Appendix: Example of Langmuir Single-Component Isotherms

In this case, a large part of the calculations may be carried out analytically, and therefore it constitutes a good illustration. Letting:

$$q_i = \frac{q_{im} k_i p_i}{1 + k_i p_i} \tag{A1}$$

the derivative is

$$\frac{dq_i}{dp_i} = \frac{q_{im}\, k_i}{(1 + k_i p_i)^2} \tag{A2}$$

and the spreading pressure or rather the loading ψ is obtained from:

$$\psi = \int_0^{P_i} \frac{q_i}{p_i} dp = q_{im} \ln(1 + k_i p_i) \tag{A3}$$

For a given loading ψ, Eq. (A3) may be inverted to yield:

$$p_i = \frac{-1}{k_i}\left[1 - \exp\left(\frac{\psi}{q_{im}}\right)\right] \tag{A4}$$

In mixture adsorption, the value of spreading pressure or loading is common to all components, and therefore, for a given value of ψ, the fictitious pressures P_i^* of all components must have values that satisfy Eq. (A3) or (A4).

The "curvature parameters" ξ_i are given by Eq. (A5) below and may be computed, using Eqs. (A1) and (A2).

$$\xi_i^* = \frac{P_i^*}{q_i}\left(\frac{dq_i}{dp_i}\right)_{p=P_i^*} = \frac{1}{1 + k_i P_i^*} \tag{A5}$$

The limiting values at infinite dilution of component 1 may be calculated by observing that when $x_1 \to 0$, $p_2 \to P$, $P_2^* \to P$ and $q_2 \to q_2(P)$. Then Eq. (A3) is written twice for $i = 1$ and 2, and the right hand sides are equated and solved for $P_{1\,\mathrm{lim}}^*$ to give:

$$P_{1\,\mathrm{lim}}^* = \frac{1}{k_1}\left[-1 + [1 + k_1 P]^{\frac{q_{2m}}{q_{1m}}}\right] \tag{A6}$$

The limit value $q_{1\,\mathrm{lim}}^*$ necessary to use Eqs. (2), (28), (29) is then obtained from the isotherm Eq. (A1):

$$q_{1\,\mathrm{lim}}^* = q_1(P_{1\,\mathrm{lim}}^*) = \frac{q_{1m} k_1 P_{1\,\mathrm{lim}}^*}{1 + k_1 P_{1\,\mathrm{lim}}^*} \tag{A7}$$

Finally, Eq. (A5) is particularized for $i = 2$, with $P_2^* = P$:

$$\xi_{2\,\mathrm{lim}}^* = \frac{1}{1 + k_2 P} \tag{A8}$$

All quantities involved in Eqs. (28) and (29) have now an explicit algebraic expression, calculable from the single component isotherms, and therefore the "theoretical IAS value" of dm_t/dp_1 may be calculated, and compared to the measured value. Of course, the same procedure is used for infinite dilution of component 2. If the discrepancy between measured and calculated values of dm_t/dp_1 justifies it, γ_i^∞ is used as adjusting parameter in Eqs. (38)–(40), all other quantities being constant. With two values of γ^∞ and a classical two parameter model of activity coefficients, the RAS approach is then completely identified. If one wants to test the two parameter SPD model, Eq. (60) is used with ψ_{lim} calculated from Eq. (A3) as

$$\psi_{\mathrm{lim}}(x_1 \to 0) = q_{2\mathrm{m}} \ln(1 + k_2 P) \tag{A9}$$

The constants B and C are identified and reintroduced into Eq. (54), completing the identification of this model.

Nomenclature

a_i	Molar surface area of species i ($m^2\ mol^{-1}$)
A	Specific surface area of adsorbent ($m^2\ kg^{-1}$)
B	Coefficient in ISAC model (Eq. (53)–(60)) ($J \cdot mol^{-1}$)
C	Coefficient in ISAC model (Eq. (53)–(60)) ($kg \cdot mol^{-1}$)
g	Molar Gibbs energy ($J \cdot mol^{-1}$)
g^{ex}	Excess molar Gibbs energy in adsorbed phase ($J \cdot mol^{-1}$)
k_i	Coefficient in Langmuir isotherm (Eq. (60)) (bar^{-1})
G^{ex}	Excess Gibbs energy of adsorbed phase (J)
m	Coefficient in Flory-Huggins model (–)
m_a	Mass of clean adsorbent sample (kg)
m_i	Adsorbed mass of component i (kg)
m_t	Total adsorbed mass (kg)
M	Average molar mass of the gas mixture ($kg \cdot mol^{-1}$)
M_i	Molar mass of component i ($kg \cdot mol^{-1}$)
$M_2^{'RAS}$	Quantity defined in Eq. (39) ($kg \cdot mol^{-1}$)
$M_2^{'SPD}$	Quantity defined in Eq. (51) ($kg \cdot mol^{-1}$)
n	Number of moles of the mixture (mol)
P_i	Partial pressure of component i in gas (Pa) or (bar)
P	Total pressure (Pa) or (bar)
P_i*	Fictitious pressure of component i in Adsorbed Solution theory (Pa) or (bar)
q_i	Concentration of adsorbed component i ($mol \cdot kg^{-1}$ adsorbent)
q_m	Maximal adsorbed concentration in Langmuir isotherm ($mol \cdot kg^{-1}$)
q_t	Total concentration in adsorbed phase ($mol \cdot kg^{-1}$)
Q	Coefficient in Eq. (40), defined by Eq. (41) ($kg \cdot bar^{-1}$)
R	Coefficient in Eq. (40), defined by Eq. (41) ($kg \cdot bar^{-1}$)
R	Gas constant ($J \cdot mol^{-1} \cdot K^{-1}$)
S^{ex}	Excess entropy of mixing in adsorbed phase ($J \cdot K^{-1}$)
T	Temperature (K)
V^{ex}	Volume of mixing in the adsorbed phase (m^3)
x_i	Mole fraction of component i in adsorbed phase (–)
y_i	Mole fraction of component i in gas phase (–)

Greek Letters

α	Coefficient in Van Laar model (–)
α_i	Coefficient in Margules model (–)
β	Coefficient in Van Laar model (–)
β_i	Coefficient in Margules model (–)
γ_i	Activity coefficient of component i in adsorbed phase (–)
Δ	Defined by Eq. (35) or (47) (–)
Δ_i	Quantity defined in Eq. (46) (–)
Δ_2'	Quantity defined in Eq. (52) ($kg \cdot mol^{-1}$)
Λ_{12}, Λ_{21}	Parameters of Wilson model (–)
χ	Parameter of Flory-Huggins model (–)
Π	Spreading pressure of adsorbed phase ($J \cdot m^{-2}$) or ($N \cdot m^{-1}$)
ψ	Loading, or compressibility factor of adsorbed phase ($mol \cdot kg^{-1}$)
ξ_i	Concavity parameter of isotherm of component i, defined by Eq. (24) (–)

Subscripts

1, 2	Designate components 1 (CO_2) and 2 (CH_4)
i, j	Designate components
lim	Designates limiting values, when the concentration of one component tends toward zero
t	Designates total quantities, sum of the quantities relative to the two components

Superscripts

ex	Excess properties
$*$	Properties of single component equilibria
$\circ$	Initial state
∞	Infinite dilution
$-$	Overline—partial molar quantities

Acknowledgments

This work was carried out in the framework of the research program CARBMAT, supported by the French Ministry of Research, under the coordination of the Company L'Air Liquide, Centre de Recherches Claude-Delorme, Les-Loges-en-Josas, France. The authors are grateful to the Company for financing the thesis of K. Bonnot and for providing adsorbents and data, and to the researchers of the Centre de Recherches

who participated in the program, for fruitful discussion, constructive criticism and efficient coordination. We specially thank Dr Lianming SUN for starting this co-operation and for his scientific advice. We would also like to thank the researchers of Institut des Matériaux et Procédés du CNRS in Perpignan, France, as co-participants to the program.

References

Abrams, D.S. and J.M. Prausnitz, "Statistical Thermodynamics of Liquid Mixtures: A New Expression for Excess Gibbs Energy of Partly or Completely Miscible Systems," *A.I.Ch.E.J.,* **21**, 116 (1975).

Buss, E., "Gravimetric Measurements of Binary Equilibria of Methane-Carbon Dioxide Mixtures on Activated Carbon," *Gas Sep.Purif.*, **9**, 189–197 (1995).

Costa, E., J.L. Sotelo, G. Calleja, and C. Marron, "Adsorption of Binary and Ternary Hydrocarbon Gas Mixtures on Activated Carbon: Experimental Determination and Theoretical Prediction of the Ternary Equilibrium Data," *A.I.Ch.E.J.*, **27**, 5–12 (1981).

Do, D.D., *Adsorption Analysis: Equilibrium and Kinetics*, Imperial College Press, London 1998.

Dreisbach, F., R. Seif , H. Lösch, and J.U. Keller, "Gravimetric Measurement of Adsorption Equilibria of Gas Mixtures CO/H_2 with a Magnetic Suspension Balance," in *Proc.7th Conf. Fundamentals of Adsorption*, K. Kaneko and Y. Hanzawa, Eds., pp. 255–262, J.K International, Chiba, Japan, 2001.

Friedrichs, R.O. and J.C. Mullins, "Adsorption Equilibria of Binary Hydrocarbon Mixtures on Homogeneous Carbon Black at 25°C," *Ind. Eng. Chem. Fundam*. **11**, 439–445 (1972).

Herington, E.F., "A Thermodynamic Test for the Internal Consistency of Experimental Data on Volatility Ratios," *Nature*, **160**, 610–611 (1947).

Kabir, H., G. Grevillot, and D. Tondeur, "Equilibria and Activity Coefficients for Non-Ideal Adsorbed Mixtures from Perturbation Chromatography," *Chem. Eng. Sci.*, **53**(9), 1639–1654 (1998).

Keller, J.U., F. Dreisbach, H. Rave, R. Staudt, and M. Tomalla, "Measurement of Gas Mixture Adsorption Equilibria of Natural Gas Compounds on Microporous Adsorbents," *Adsorption*, **5**, 199–214 (1999).

Kopatsis A., A. Salinger, and A.L. Myers, "Thermodynamics of Solutions with Solvent and Solute in Different Pure States," *A.I.Ch.E.J.*, **34**, 1275–1286 (1988).

Myers, A.L., "Gravimetric Measurement of Adsorption from Binary Gas Mixtures," *Pure & Appl. Chem.*, **61**, 1949–1953 (1989).

Myers, A.L., C. Minka, and D.Y. Ou, "Thermodynamic Properties of Adsorbed Mixtures of Benzene and Cyclohexane on Graphitised Carbon and Activated Charcoal at 30°C," *A.I.Ch.E.J.,* **28**, 97–102 (1982).

Myers, A.L. and J.M. Prausnitz, "Thermodynamics of Mixed Gas Adsorption," *A.I.Ch.E.J.*, **11**, 121–127 (1965).

Renon, H. and J.M. Prausnitz, *A.I.Ch.E.J.*, **14**, 135 (1968).

Sandler, S.I., *Chemical and Engineering Thermodynamics,* Wiley, New-York, 1999.

Siperstein, F., R.J. Gorte, and A.L. Myers, "Measurement of Excess Functions of Binary Gas Mixtures Adsorbed in Zeolites by Adsorption Calorimetry," *Adsorption*, **5**, 169–176 (1999).

Talu, O. and I. Zwiebel, "Multicomponent Adsorption Equilibria of Non-Ideal Mixtures," *A.I.Ch.E.J.,* **32**, 1263– (1986).

Van der Vaart, R., C. Huiskes, H. Bosch, and T. Reith, "Single and Mixed Gas Adsorption Equilibria of Carbon Dioxide/Methane on Activated Carbon," *Adsorption*, **6**, 313–323 (2000).

Van Ness, H.C., "Adsorption of Gases on Solids," *I&EC Fundam.,* **8**(3), 464–473 (1969).